ASHA American Speech-Language-Hearing Association

JSLHR

Research Article

The Compartmental Tongue

Alan A. Wrench[a,b]

[a] Queen Margaret University, Edinburgh, United Kingdom [b] Articulate Instruments Ltd, Edinburgh, United Kingdom

ARTICLE INFO

Article History:
Received February 17, 2023
Revision received June 25, 2023
Accepted March 8, 2024

Editor-in-Chief: Ben A. M. Maassen
Editor: Philip Hoole

https://doi.org/10.1044/2024_JSLHR-23-00125

ABSTRACT

Purpose: Tongue anatomy and function is widely described as consisting of four extrinsic muscles to control position and four intrinsic muscles to control shape. This myoarchitecture cannot, however, explain independent tongue body and blade movement nor accurately model the subtlety of observed lingual shapes. This study presents the case for a finer neuromuscular structure and functional description.
Method: Using the theoretical framework of the partitioning hypothesis, evidence for neuromuscular compartments of each of the lingual muscles was discerned by reviewing studies of lingual anatomy, hypoglossal nerve staining, hypoglossal motoneuron axon tracing, muscle fiber type distribution, and electromyography. Muscle fibers of the visible human female were manually traced to produce a three-dimensional atlas of muscular compartments. A kinematic study was undertaken to determine the degree of independent movement between different parts of the tongue. A simple biomechanical model was used to demonstrate how synergistic groups of compartments can control sectors of the tongue.
Results: Results indicated as many as 10 compartments of genioglossus, two each of superior and inferior longitudinal, eight of styloglossus, three of hyoglossus, and six each of transversus and verticalis, while palatoglossus may not have a significant role in tongue function. Kinematic analysis indicated independent control of five sectors of the tongue body, and biomechanical modeling demonstrated how this control may be achieved.
Conclusion: Evidence is presented for a lingual structure based on neuromuscular compartments, which work together to position and shape sectors of the tongue and independently control tongue body and blade.

Both speech and swallowing require shaping and positioning of the tongue. In speech, the different vowel sounds are produced by changing the shape of the midsagittal portion of the tongue. Velar stops require the tongue body to form a constriction with the palate. When swallowing liquid, the tongue body must make a seal with the palate to prevent premature anterior to pharyngeal transition of the bolus while, at the same time, the tongue blade manipulates and transports the bolus posteriorly. These speech and swallowing actions require subtle, fine control of different parts of the tongue.

Correspondence to Alan A. Wrench: awrench@articulateinstruments.com. **Publisher Note:** This article is part of the Special Issue: Select Papers From the 8th International Conference on Speech Motor Control. ***Disclosure:*** *The author has declared that no competing financial or nonfinancial interests existed at the time of publication.*

Descriptions of how the tongue functions are to be found in most anatomy texts. These descriptions assign functions to a set of eight muscles of the tongue, which are officially recognized by the Federative International Programme for Anatomical Terminology (FIPAT) in the Terminologia Anatomica (FIPAT, 2019):

- genioglossus muscle
- hyoglossus muscle
  - chondroglossus muscle (zone of hyoglossus)
  - ceratoglossus muscle (zone of hyoglossus)
- styloglossus muscle
- palatoglossus
- superior longitudinal lingual muscle
- inferior longitudinal lingual muscle

- transversus linguae muscle
- verticalis linguae muscle

The eight muscles are classified as extrinsic or intrinsic. A typical description of the function of those muscles is provided in Gray's Anatomy (Standring, 2021).

Extrinsic muscles are described as follows. "The genioglossus muscles depress the central part of the tongue and protrude the anterior part of the tongue out of the oral fissure." "The styloglossus muscles retract the tongue and pull the back of the tongue superiorly." "The hyoglossus muscle depresses the tongue." "The palatoglossus muscles elevate the back of the tongue."

Intrinsic muscles are described in the following terms. Superior longitudinal "shortens the tongue; curls apex and sides of tongue." Inferior longitudinalis "shortens tongue; uncurls apex and turns it downwards." Transversus "narrows and elongates tongue." Verticalis "flattens and widens tongue." In summary, the conventional description of lingual function holds that the extrinsic muscles position the tongue and the intrinsic muscles act to shape the tongue (Standring, 2021; Sutlive et al., 1999).

There is, however, limited evidence to support these broad functional claims, which appear to be largely based upon the line of action of the muscle fibers, and electromyography (EMG) studies, which show styloglossus activity for velar and high back vowel articulation and hyoglossus activity for low back vowels (Baer et al., 1988; Waltl & Hoole, 2008). EMG studies of palatoglossus during speech have found no consistent relationship between tongue raising and activation of this muscle (Fritzell, 1969; Kuehn & Azzam, 1978; Lubker et al., 1973).

The careful observation of tongue movements either directly or via imaging techniques such as magnetic resonance imaging (MRI) and ultrasound also reveals discrepancies in these descriptions. For example, tongue bunching can be produced without pulling the tongue up and back; that is, the tongue can be bunched while the tip remains in the same location. Styloglossus as a single neuromuscular unit extending from the styloid process to the tongue tip cannot achieve this and must therefore either have at least two neuromuscular compartments (NMCs) capable of independent control or not be involved in tongue retraction. When the function of genioglossus is observed in breathing, swallowing, and speech, it is most often divided into two (Mu & Sanders, 2010) or three (Gérard et al., 2003; Takano & Honda, 2007) independent functional compartments in order to explain observed changes in shape. However, if the genioglossus must be divided into at least three functional compartments, this seems arbitrary, why not four, five, or more.

For those that have studied this complex organ in detail, intrinsic and extrinsic categorization is of "no proper scientific significance" (Abd-el-Malek, 1938; Schwenk, 2001) aside, perhaps, from acting as an aide memoire for students of anatomy. Sokoloff and Burkholder (2013) conclude that "conventional definitions of tongue muscles do not offer sufficient anatomical resolution to account for regionally diverse deformations of the tongue body. Extrinsic and intrinsic tongue muscles have complex and distributed muscle fibre architecture and motor units localized within the tongue body. These features suggest that tongue deformation may be determined by the differential activation of motor units by orientation and region (and not by muscle or compartment membership per se)." Liu (2012) agrees, concluding "the tongue motor control most likely uses grouped motor unit- or segmented structure unit-based, rather than entirely muscle-based strategies."

Sakamoto (2018) also finds that "the intrinsic and extrinsic muscles of the tongue are not independent groups, and their fibres form a three-dimensional (3D) latticework. Each muscle contains numerous bundles or lamellae as functional units that can act separately or cooperate across the muscles."

The key to a better understanding of tongue function is to realize that a muscle is not a fundamental neuromuscular unit. Many, if not the majority of, skeletal muscles in the human body consist of NMCs, each with individual primary nerve innervation capable of independent contraction. "Compartmentalization often is most apparent in muscles with spatially distributed origins and/or insertions. Although the different compartments of such a muscle typically have similar histochemical fibre-type composition, their different origins and/or insertions give contraction of each compartment a different biomechanical effect" (Chanaud et al., 1991).

However, there is no atlas of this fine structure for the human tongue available to present to students of speech and swallowing science. This article seeks to address this by producing a 3D atlas along with supporting evidence and proposes how synergistic groups of NMCs may work together to form the necessary shapes and functions.

Compartmentalization of Muscles and Their Motor Nuclei: The Partitioning Hypothesis

The partitioning hypothesis is a theory of neuromuscular control proposed by English et al. (1993) based upon observations by English (English & Weeks, 1984) and others (Windhorst et al., 1989). The theory holds that an

NMC is the smallest portion of a muscle that receives exclusive innervation by a group of motoneurons. Such a portion can be contracted independently of other portions of the same muscle. There are several key indicators of an NMC.

- The axon of any motoneuron in the motor nucleus should extend to one and only one compartment. The condition is most often met at the level of primary nerve twigs. Primary or first-order branches of the muscle nerve are usually the last major subdivision of the nerve before it divides into multiple small twiglets, which pass to the end-plate region of the muscle fibers. The number and location of primary nerve branches is therefore an indicator of the number and location of NMCs.
- Since motoneurons innervate muscle fibers of only a single histochemical type, an indication of separate compartments is regions of a muscle containing different proportions of fast and slow fibers. We will see evidence that the superior longitudinal muscle has distinctive proportions of fiber types medially compared with laterally.
- The groups of motoneurons associated with an NMC, rather than being distributed widely within the motor nucleus, tend to be located proximately to each other and each group arranged musculotopically. We will see evidence that genioglossus muscle afferents are arranged along the length of the cylindrical hypoglossal nucleus in a spatial order that corresponds to the position of compartments arranged from anterior to posterior.
- Fiber bundles making up a compartment may share an origin (or head) in the case where they originate from a bone or tendon (e.g., the chondroglossus and ceratoglossus parts of the hyoglossus have distinct origins). Or, where they do not attach to a bone, they share a common direction so as to provide a localized function. We will see that the inferior longitudinal muscle has two distinct orientations of fibers.

The theory of NMCs is not controversial, but the extent of this compartmentalization may be underestimated.

English et al. (1993) ask the functional questions:

1. Are anatomically defined partitions of human muscles functional partitions?
2. Do partitions of different muscles form functional synergies?

This article will conclude that the answer to both these questions in relation to the tongue is "yes."

Modularization and Synergies

There is a widely held view (Gick & Stavness, 2013) that neuromuscular modules or proportionately fixed groupings of muscles control movements. This is seen as a way of reducing the number of degrees of freedom to simplify neural control. We will discuss how the proposed NMCs of the tongue can work together (synergize) to control shape and position. The definition of muscle synergies that we will use is described (Bizzi & Cheung, 2013) as "neurophysiological entities whose combination is orchestrated by the motorcortical areas and the afferent systems." Elsewhere, synergies have mathematical descriptions such as "movement primitives" or very broad descriptions such as "coordinative structures" and are often related to tasks. The synergies we will describe are lower level and likely to have evolved for swallowing and mastication. By good fortune, they also afford the level of fine shape control required to copy sounds made by other humans despite anatomical variation in tongue size, palate shape, mandible size, and other interpersonal differences.

Method

Sources of Evidence for NMCs

Segmentation of the Visible Human Female

The tongue consists of a complex arrangement of interlinking muscle fibers. Using traditional anatomical dissection, it is challenging to tease apart the many fibers and map their course and relationship to each other within the 3D structure. To follow one set of fibers of necessity means that the remainder of the tongue must be broken apart and the overall geometry is lost. Presentation of results of detailed anatomical studies often takes the form of a descriptive text accompanied by labeled grayscale photographs or drawings of a very localized volume. Some anatomical studies view 2D cut sections through the tongue to preserve the structure (Malpighi, 1665; Saigusa et al., 2004), but most often the 3D course of muscle fibers in the intact tongue is not observed and must be inferred.

The visible human female (VHF; Ackerman, 1998; Spitzer et al., 1996) is one of three cadavers photographically scanned and made publicly available for research in 1996. The female subject head was separated from the body, frozen in an aqueous gel then polished (cryosectioned) to reveal axial (transverse) sections stopping every 1/3 mm to take a photograph. Each photograph was digitized at a resolution of 1/3 mm = 1 pixel. Thus, a volume was created with voxels of size 1/3 × 1/3 × 1/3 mm.

The process of segmenting this digitized volumetric data requires a specialist software. Amira (Version 6.3;

Thermo Fisher Scientific) was used for this study, although other similar packages are available. Such software displays three grayscale orthogonal views of the volume. Tools are provided to allow manual highlighting of regions in these planes and to label collections of highlighted pixels. Labeled pixels can be differently colored and viewed in three dimensions. It is also possible with such software to run a 3D smoother over the surface of a given labeled volume. While smoothing makes sense for bones, cartilage, and adipose tissue with no fibrous structure and creates a pleasing smooth boundary, it is ill-advised for muscle tissue for two reasons. First, the smoothed 3D structure does not show the fiber directions. Second, it forces the user to label contiguous areas of the image rather than individual fibers because labeled areas with gaps between fibers do not smooth properly.

There are significant challenges to tracing muscle fibers. Although the VHF photographs are in color and can be viewed in color volumes, the segmentation tool is constrained to operate on grayscale luminance values. The removal of color strips away is one means of distinguishing tissue types. On occasion, it was necessary to observe the slice being segmented both in the segmentation software and separately from a color volume. While it is possible to view the volume in nonorthogonal and even curved planes, the segmentation function is limited to labeling pixels in the three orthogonal planes. It can be difficult to trace fibers that are not aligned with these planes. Not only that, but there is a tendency on the part of the labeler to see patterns within a plane that actually result from combinations of oblique fibers. To mitigate this tendency, fiber patterns were checked and corrected so that they made sense in all three orthogonal planes. Nevertheless, the transversus and verticalis fibers, which curved in all three dimensions, could not be satisfactorily traced using this software.

The VHF does have an advantage of significant deposit of white fatty (adipose) tissue interspersed with the tongue fibers, which contrast with the muscle tissue and aid in determining fiber direction. The VHF also has the advantage that the tongue is at rest (no muscles are contracted) with cricoid thyroid, hyoid, and all the supralaryngeal muscles intact.

Previous attempts have been made to trace the myoarchitecture of the tongue using the VHF subject. Wilhelms-Tricarico (2000), and Baker (2008) used the data as a reference to create 3D finite element models of the tongue. Kajee et al. (2013) and Pelteret and Reddy (2014) traced muscle fibers, again to form a basis for tongue modeling. Pelteret stated, "Due to the complexity of the tongue histology and the relative coarseness of the photographic data-set, some of the muscles did not prominently feature and could not be observed to a high degree of confidence. Guided by the literature (Abd-el-Malek, 1939; Davies & Gray, 1967; Morley, 1972; Takemoto, 2001; Agur & Dalley, 2005), the position and directionality of these muscles was inferred relative to the more visible musculature."

Iskander and Sanders (2003) and Sanders et al. (2013) used the data to segment the lingual muscles as did Sanders and Mu (2013) to provide illustrations for their atlas of the human tongue. With the exception of Kajee et al. (2013) and Pelteret and Reddy (2014), segmentation of VHF has been done by blocking and smoothing areas where each of the muscles is located. Kajee et al. attempted to use a fiber tracing tool, which can follow arteries and veins through a 3D volume, but it does not work well for fine muscle fibers.

In vivo segmentation of MRI images of the human tongue has also been produced (Stone et al., 2018; Woo et al., 2019). Recent work with MRI diffusional data (Liang et al., 2022; Taylor et al., 2015) demonstrates that this noninvasive technique can reveal 3D myofiber architecture in vivo, and these fibers can be labeled and interpreted using anatomical texts. It is not clear whether the resolution of this technique is sufficient to allow firm conclusions on the function of the tongue. To date, authors using this technique have assigned the revealed fiber tracks to one of the eight extrinsic/intrinsic muscle groups. It does not appear to be sensitive enough to distinguish NMCs.

The segmentation illustrated in this article is the result of not one but several passes over the data, ensuring that the traced segmentation made sense in all three orthogonal planes. This task was approached with knowledge of previous anatomical studies, but importantly, it was not bound by them. Rather, fibers were labeled in small homogeneous groups and gradually agglomerated into larger groupings, taking into account the origin and flow of fiber directions. Despite the care taken, there is a degree of uncertainty in whether this agglomeration is accurate, and it is possible that some groups of fibers have been incorrectly assigned. Evidence from previous detailed anatomical dissection and histological studies has been used to support some of the novel structures revealed by this process.

The Structure of the Hypoglossal Nucleus

The human hypoglossal nucleus contains approximately 11,000–15,000 motoneurons (70%) and inhibitory interneurons (30%; O'Kusky & Norman, 1992, 1995) controlling muscles of the tongue and the geniohyoid (Sokoloff & Deacon, 1992). The palatoglossus motoneurons are primarily located elsewhere, in the nucleus ambiguus

along with other muscles controlling the soft palate, pharynx, and larynx—a strong indication that this muscle is not primarily involved in tongue control. Descending signals from the motor cortex combine with afferent feedback signals in the hypoglossal nucleus to regulate the activation of the muscles. The hypoglossal nucleus is present in all mammals sending axons to the lingual muscles via the hypoglossal nerve. In humans, it is an approximately 2-cm-long structure located in the medulla oblongata. The musculotopic organization of the nucleus has been studied in the rat (Aldes, 1995; McClung & Goldberg, 1999; Sokoloff, 1993), cat (Uemura et al., 1979), dog (Uemura-Sumi et al., 1988), monkey (Sokoloff & Deacon, 1992; Uemura-Sumi et al., 1981), and rabbit (Uemura-Sumi et al., 1988) and is broadly consistent across species. It may be inferred that the human nucleus is likely to have a similar structure. The cells can be divided into medial and lateral columns.[1] Sokoloff and Deacon (1992) demonstrate a spatial musculotopic organization of hypoglossal motoneurons in monkeys (see Figure 1).

Motoneurons innervating the transversus and verticalis muscles are located in medial hypoglossal nucleus regions, motoneurons innervating the genioglossus are located in intermediate hypoglossal nucleus regions, motoneurons innervating the hyoglossus and inferior longitudinalis are located in ventrolateral hypoglossal nucleus regions, and motoneurons innervating the styloglossus and superior longitudinalis are located in dorsolateral hypoglossal nucleus regions. Motoneurons of the medial divisions of the hypoglossal nucleus innervate tongue muscles that are oriented in planes transverse to the long axis of the tongue, whereas motoneurons of the lateral divisions innervate tongue muscles that are oriented longitudinally. Sokoloff (1993) suggests that the segregation of motoneurons corresponds to the functional distinction between tongue protrusion and retrusion. However, the speech and swallowing functions require more subtle control than this. Feeding requires tongue blade control to manipulate food during mastication, followed by a propulsion of the bolus from the anterior oral cavity to the esophagus. This propulsion requires coordinated sequential activation of motoneurons in the medial division.

The medial and lateral columns can be divided into levels or tiers. Sokoloff and Deacon (1992) find a tendency for more posterior fibers of genioglossus, transversus, and verticalis to be found in the more rostral (upper) levels. The axon tracing method they used was not a precise technique. McClung and Goldberg (2002), using a more precise retrograde tracing targeted at posterior and anterior genioglossus fibers, observe in the rat two discrete

[1]In rat, cat, and dog, the neck is horizontal, and medial and lateral are referred to as ventral and dorsal, respectively.

Figure 1. Adapted with permission of John Wiley and Sons, Inc., from Sokoloff and Deacon (1992). A diagram of the columns and levels of the hypoglossal nucleus in a monkey showing the musculotopic organization. Posterior fibers of genioglossus are associated with motoneurons in the rostral levels, while anterior fibers are discretely associated with more caudal levels.

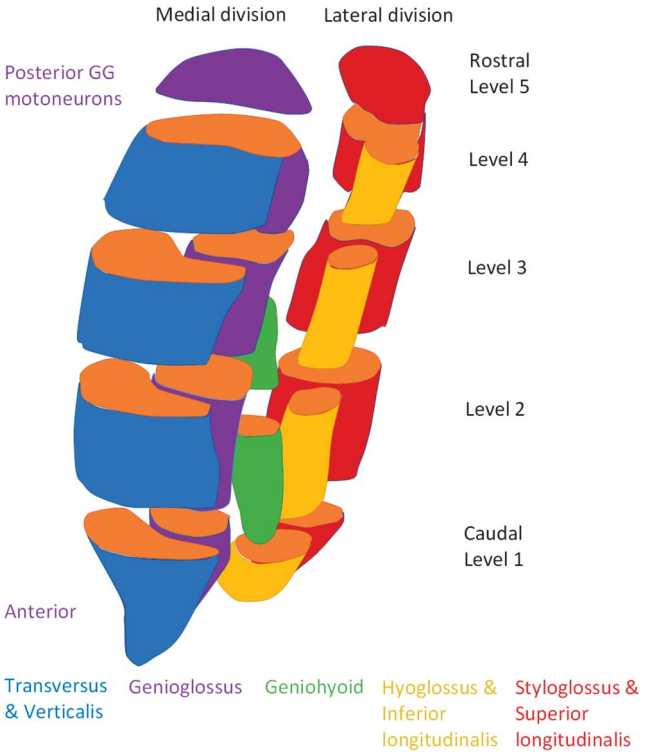

clusters of motoneurons. Again, the posterior fibers are associated with motoneurons located in a rostral region while anterior fibers map to a distinct, more caudal region of the medial column. They conclude that their retrograde label data "supports the premise that the functional organization of the tongue is best defined by specific groups of motoneurons."

Muscle Innervation by the Hypoglossal Nerve

Mu and Sanders (2010) use Sihler staining to identify branches, twigs, and muscle attachment points (end plates) of the hypoglossal nerve. Primary nerve twigs are one of the most important indicators of an NMC, and their observations will be commented upon as each muscle is discussed in the following section.

Sakamoto (2019) used dissection to follow the path of the hypoglossal nerve. He describes the nerve throwing off a branch to the posterior hyoglossus and then a cluster of branches forming a plexus (interlinked network) around the anterior part of the hyoglossus (basioglossus). Branches exiting from this plexus proceed to innervate the inferior (horizontal) genioglossus (GGh), occasionally the anterior (oblique; GGo) part of the genioglossus, and the inferior longitudinal. The main branch continues beyond the plexus

to innervate the rest of the GGo, transversus and verticalis. Ogata et al. (2002) observed that the chondroglossus was innervated by a twig from the first lateral branch of the hypoglossal nerve. The same branch also supplied the hyoglossus and styloglossus and communicated with other branches.

Muscle Fiber Type Distribution

Skeletal muscle consists of fast- and slow-type fibers. These are typically randomly distributed throughout a muscle with a percentage of each type of fiber. If a muscle has NMCs, then each NMC may have a different percentage of fiber types. Slow (Type I) contracting fibers have properties of precise control and fatigue resistance. Fast (Type II) fibers provide rapid contraction and greater force.

EMG

EMG of tongue muscles is carried out using fine wire electrodes or tungsten rods inserted percutaneously. Studies target either individual motor units or whole muscles.

Bailey (2011) reports that motor unit respiratory-related studies conducted in human subjects have documented that genioglossus appears localized in "pockets" of activity in the posterior tongue and concludes that muscles may not be the building blocks of pharyngeal movement and that pharyngeal airway lumen and stiffness may be controlled at the level of muscle compartments. The challenges of recording EMG data during speech are great, and consequently, only a few influential studies have been completed, notably by Miyawaki et al. (1975), Hirose et al. (1979), Baer et al. (1988), and Waltl and Hoole (2008).

It should be noted that EMG activity can be the result of reflexive responses as well as descending motor commands. Also, the electrodes are inserted into whole muscles so the specific NMC being recorded is unspecified.

Kinematics

Eleven key points along the midsagittal surface of the tongue were estimated from ultrasound images using the DeepLabCut (Nath et al., 2019) pose estimation method (Wrench & Balch-Tomes, 2022). DeepLabCut pose estimation was trained on approximately 2,000 hand-labeled ultrasound images of speech and water swallows from five different ultrasound systems, seven different probe geometries, and child and adult speakers. Fourteen key points are labeled: 11 points on the tongue, one on the hyoid, one on the base of the mandible (inferior tubercle), and one on the short tendon (superior tubercle; see Figure 3). Caution should be exercised in interpreting these data. Points 1 and 11 can be indistinct in ultrasound data, and sometimes the position of neighboring points may influence the estimation of their position. In other words, it is possible that the estimation process may introduce a correlation effect.

From root to tip, the first seven key points indicate the tongue body, and the last four indicate the blade/tip. For the purpose of this study, the tongue body contour from Key Points 1–7 (see Figure 3) is then interpolated along its length to extract five equally spaced points to represent five NMCs and labeled GG1 (root) to GG5 (anterior tongue body; see Figure 2). Distances from these five points to the origin of the short tendon on the superior tubercle of the mandible are then recorded for each consecutive ultrasound frame at a rate of 81 Hz.

Validity of the pose-estimated lingual key points was evaluated on a coregistered data set with electromagnetic articulograph (EMA; 200 Hz) dorsum, blade, and tip

Figure 2. Tongue spline (generated from 11 pose-estimated key points) and short tendon key points superimposed on the source ultrasound image. Distances GG1–GG5 are measured from the short tendon to five points along the surface of the tongue body. These five points are equidistant along the spline curve between the first and seventh pose estimation key points.

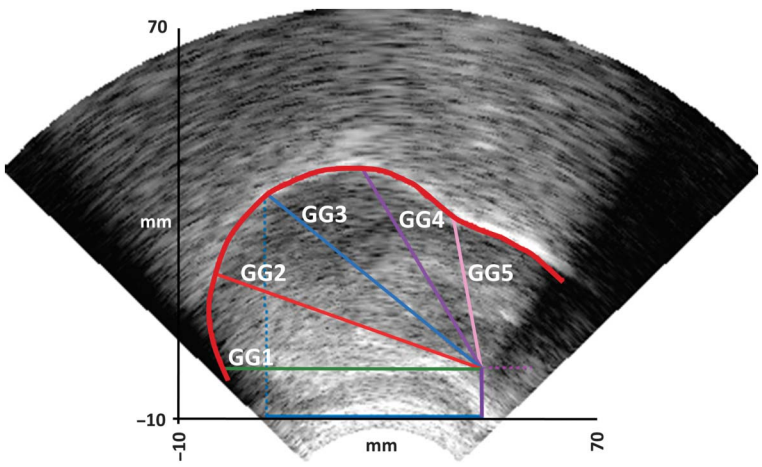

Figure 3. Sagittal diagram of the tongue with 11 pose estimation key points marked on the tongue contour, one on the hyoid, and one on each of the superior and inferior tubercles of the mandible. Three labeled key points are selected for correlation comparison with coregistered EMA data. EMA = electromagnetic articulograph.

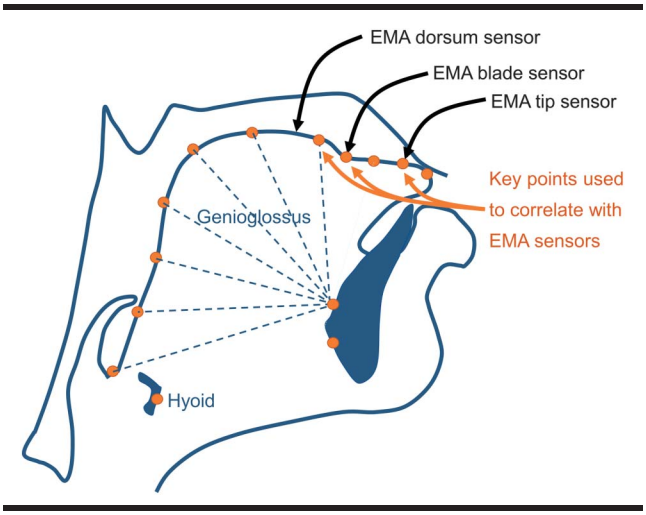

sensors and synchronous ultrasound images (81 Hz). Both systems recorded data in millimeters, and the pose-estimated data were rotated and translated to match the EMA data. The EMA sensors were correlated with the nearest pose-estimated key points (see Figure 3) for around 700 ultrasound frames taken from three phonetically balanced sentences from a single speaker (unseen in the pose estimation training set). Table 1 shows the x and y Pearson correlation scores. Y correlations are high ($> .80$). X correlations are lower due to challenges in accurately training the tip position, which is not always visible in the ultrasound image.

Results

In this section, genioglossus, hyoglossus, styloglossus, palatoglossus, inferior longitudinal, superior longitudinal, verticalis, and transversus muscles are considered in turn. Sources of evidence are presented for division of each muscle into compartments in accordance with the criteria laid out in the partitioning hypothesis. First-hand evidence is derived from careful manual segmentation of the VHF, a kinematic analysis of points along the midsagittal tongue surface, and biomechanical modeling. Kinematic analysis is applied to the midsagittal contour of the tongue to determine the degree of independent doming and grooving of different sectors of the tongue. An understanding of how this new myoarchitecture might facilitate fine functional control without necessarily increasing the degrees of freedom is important. A proposal for how individual sectors of the tongue can be grooved and domed by a synergistic combination of genioglossus, transversus, and verticalis is tested using a simple biomechanical model. This work is supplemented by evidence based on observations derived from cadaveric dissection by anatomists, which indicate both consistency and variations in myoarchitecture between individuals. Also, evidence from nerve staining of the location and number of primary hypoglossal nerve branches is collated.

Table 1. Pearson correlation scores for tongue tip, blade, and dorsum electromagnetic articulograph sensors versus closest pose-estimated key points derived from coregistered ultrasound images.

Axis	Tip	Blade	Dorsum
x	.46	.59	.67
y	.81	.88	.91

Anatomical Evidence for Compartmentalization of Individual Muscles

Genioglossus

The compartmentalization of the genioglossus is arguably the key to unlocking the structure and function of the tongue. Genioglossus fiber bundles arise from a short tendon attached to the superior mental spine (or tubercle) located midsagittally on the mandible. These fiber bundles fan out from this tendon, with anterior fibers coursing superiorly to the anterior tongue body and posteriorly toward the hyoid and distributed evenly in between. There is some disagreement about whether the anterior fibers extend into the tip. Miyawaki et al. (1975) observe that genioglossus fibers are not found to curve anteriorly into the tip. There are also conflicting reports of a few posterior genioglossus fibers extending to the hyoid, pharynx, and epiglottis. Zaglas (1850) dismisses such accounts, stating, "As Blandin has well observed, none of the fibres of this muscle ascend to the pharynx, and none are attached to the hyoid bone; the supposition that they do, being an illusion produced by the penetration of some fasciculi through the chondroglossus, or by the strong fascia stretched between the bone and the muscle." Sakamoto (2018) disagrees, stating that "the inferior fibres of the most inferior part were directed to the epiglottis and the hyoid bone."

Genioglossus exhibits variation in fiber type distribution from anterior to posterior. Sanders et al. (2013) noted the genioglossus had 46% slow-type fibers anteriorly, 59% in the body and 64% in the base of the tongue. Precise locations are not indicated.

The idea that the genioglossus might be constructed from many fascicles (bundles of fibers surrounded by a thin sheath of perimysium) is raised very early on. Crooke (1615), translating Bauhini quoting Vesalius, states, "They

[genuoglossi] haue also certaine lines in them which anatomists call inscriptions as if they were many muscles." Sakamoto (2017) observes 20–25 fascicles separated by thin perimysium.

Most often the genioglossus is described in modern textbooks as consisting of two functional compartments: a horizontal compartment (GGh) originating from the inferior part of the short tendon affecting the pharyngeal cavity and an oblique compartment (GGo) affecting the oral cavity. Biomechanical modelers (Dang & Honda, 1997; Hermant et al., 2017; Wrench & Balch, 2015) find it necessary to divide the genioglossus into at least three compartments to model tongue shapes. Mu and Sanders (2010) study human cadavers and identify two primary hypoglossal nerve twigs leading to GGh (see Figure 4, lines A and B) and GGo (see Figure 4, lines C, D, and E) parts. They also identify two to three secondary nerve branches to GGh and five to six secondary branches to GGo. Although termed "secondary," these nerve twigs are clearly first order and innervate distinct regions of the genioglossus (see Figure 6B in Mu & Sanders, 2010). In an earlier work on the canine tongue (Mu & Sanders, 1999), they observed 10 nerve twigs serving the genioglossus with three to four primary twigs to GGh and seven to eight to GGo. In a personal communication with Liancai Mu (personal communication, 2014), he further proposed, "The human GG appears to be composed of at least 4 NMCs, including GGh and 3 GGo sub-compartments while considering muscle fibre arrangement, fibre type distribution (regionalization), and nerve supply patterns. These anatomically and histochemically defined compartments may have differences in EMG muscle activities during speech, swallowing and respiratory motor tasks. It is possible the GG is composed of 5 or more NMCs given its innervation by 6–7 first-ordered branches."

Figure 4. Sagittal view of the tongue with five paired compartments of the genioglossus. Orange lines define planes of the five transverse slices (A–E) through the tongue body and one slice (F) through the tongue blade, as illustrated in Figure 5.

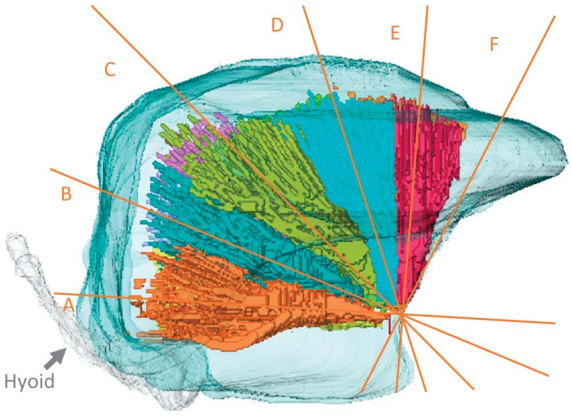

Miyawaki et al. (1975) conducted a canine experiment where they stimulated four primary nerve twigs serving the medioposterior region of the genioglossus and observed distinct localized contractions. In the same article, they report inserting EMG needles into five distinct regions of the human genioglossus and observing distinct EMG patterns from each region. Delaey et al. (2017) used dissection of 15 adult cadavers bilaterally and found an average of 4.9 primary nerves (±1.3).

Saigusa et al. (2001) observe that the muscle fibers in GGh have the largest diameter, with the diameter gradually diminishing for the more anterior fibers. It would therefore appear to be the case that the larger volume of the posterior genioglossus NMCs indicated in Figure 6 is due to fiber diameter rather than a greater number of fibers. The larger diameter may be required as the posterior fibers are working against the weight of the anterior tongue mass under typical upright or supine posture. More powerful contractions are therefore required in this region.

Yeung et al. (2022) use hook wire electrodes in 63 participants to examine genioglossus activation during swallowing. They place two electrodes in the horizontal part (GGh) and two in the oblique part (GGo). They observe anterior compartments activate 75 ms before posterior compartments, concluding this is likely to be a peristaltic-like action by independently controlled compartments of the genioglossus.

In this study, careful segmentation of the VHF revealed approximately 10 points of origin around the short tendon from which fibers radiated. These fiber groupings were arranged in five sectors, each with a medial and lateral compartment (see Figure 6). The GGh region contains two of the five sectors (see Figure 4, lines A and B), while the remaining three sectors lie in the GGo region (see Figure 4, lines C, D, and E) and correspond to the three NMCs proposed by Mu (personal communication, 2014).

Hyoglossus

There are three well-documented muscular compartments connecting the hyoid to the tongue:

- basioglossus with origin from the body of the hyoid and insertion at the lateral margin of the tongue,
- ceratoglossus with origin from the greater cornu and insertion at the posterior margin of the tongue, and
- chondroglossus with origin from lesser cornu and insertion at the posterior dorsum of the tongue.

As a result of confusion created by Vesalius, the ceratoglossus and basioglossus compartments of the hyoglossus

Figure 5. Five transverse slices (A, B, C, D, and E) through the tongue body and a sixth slice through the tongue blade. See Figure 4 for the orientation of each slice. Slices A–D show each genioglossus muscle has two rows of fiber bundles. Transverse muscle fibers insert into the lateral dorsum of the tongue in the three anterior slices D, E, and F. In the posterior two slices (A and B), the transverse fibers are extensions of the styloglossus forming a stirrup. Slice 3 may also be partially blended with a compartment of styloglossus. Two bundles of genioglossus fibers can be seen on the left side of each transverse section (most clearly in C), which reveal two rows of compartments in each genioglossus muscle.

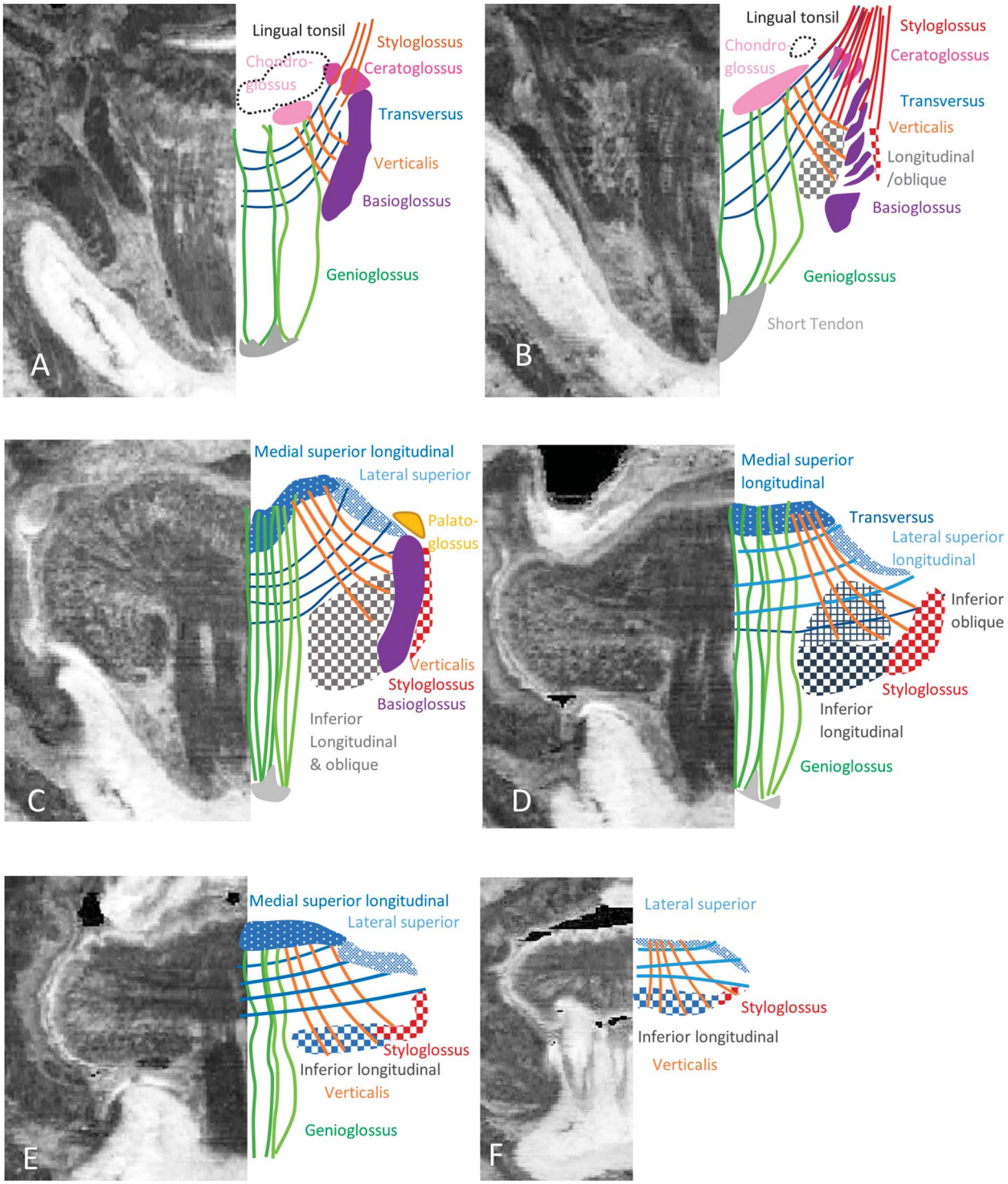

Figure 6. Neuromuscular compartments of the genioglossus in two rows of five compartments. (a) Sagittal view of medial row. (b) Sagittal view of lateral row. (c) Axial view from above. Ten compartments from one of the two genioglossus muscles are shown.

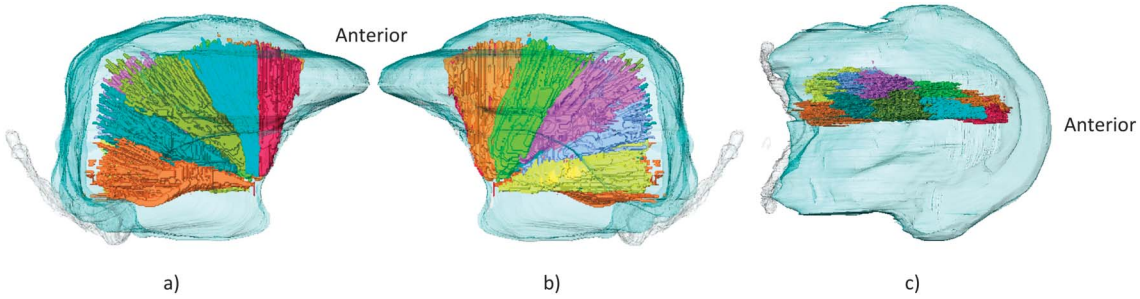

have been consistently observed, described, and named from 1605 onward. "Ceratoglossus" remains an officially recognized term for this zone of the hyoglossus (FIPAT, 2019), but the term "basioglossus" is no longer officially recognized, although it is occasionally referred to (Sakamoto, 2017, 2018; Tubbs et al., 2016).

The chondroglossus was first recorded by the Flemish anatomist Verheyen (1710). He specifies the chondroglossus as the fifth of six pairs of lingual muscles. Ogata et al. (2002) carried out a detailed review of the history of the chondroglossus and examined 100 cadaveric tongues from the Japanese population. They concluded that it could be found in every tongue. They report that it arises from the lesser horn of the hyoid, penetrates the inferior longitudinal muscle near its origin, and then fans out through posterior genioglossus fibers, terminating diffusely in the submucosal layer of the root of the tongue posterior to the sulcus terminalis. It should be noted that this is also the origin of the superior longitudinal muscle. Ogata et al. consider that the chondroglossus is not part of the hyoglossus but a separate muscle as it has a distinct origin and has a different function.

Chondroglossus is innervated by a single twig from one of the lateral branches of the hypoglossal nerve (Ogata et al., 2002). There are no explicit reports of distinct innervation of ceratoglossus and basioglossus, but Figure 5 in Mu and Sanders (2010) shows at least two primary nerve twigs entering the hyoglossus at locations commensurate with these two compartments. Compartments of the hyoglossus are shown in Figure 7.

Styloglossus

The historical record reveals proposed compartments of the styloglossus as early as 1844. Cruveilhier (1844) in his *Anatomy of the Human Body* describes the styloglossus as dividing into two parts: one external, which runs along the corresponding margin of the tongue from the base to the apex, and the other internal, which passes between the two portions of the hyoglossus, assumes a transverse direction, and is blended with the transverse fibers of the tongue. Albert von Koelliker (1851) similarly distinguishes two parts. Salter (1852) proposed that the fibers running along the lateral margin of the tongue be considered two "lateral longitudinal" muscles, although he considers one deriving from styloglossus and the other from hyoglossus. Dabelow (1951) and Saito and Itoh (2007) carry out detailed studies finding two parts, one extending laterally as longitudinal fibers in a slight curve forward to the tip of the tongue and the other interdigitates with the hyoglossus and continues medially and anteriorly to terminate at the median septum, forming a sling. Saito and Itoh (2007) describe the fibers entering the tongue body as dividing into 10 bundles and having a multilayer structure. Takemoto (2001) and Barnwell (1977) observe a third bundle of posterior fibers that intersect with the hyoglossus. Jonnesco (1902) describes the fibers passing through the ceratotoglossus, or between it and the basioglossus, as dividing into two or three distinct bundles before intersecting with inferior longitudinal as they penetrate the root.

Sakamoto (2017) examines 42 cadavers finding that styloglossus has three bundles of fibers each with distinguishable superficial and deep parts, making six compartments in total. He assigns the initial three bundles as an exterior bundle passing the hyoglossus on the outside, an interior bundle passing the hyoglossus on the inside, and a medial bundle passing between the anterior and posterior parts of the hyoglossus, which he refers to as basioglossus and ceratoglossus. The superficial fibers of the exterior bundle extend along the periphery to insert into the tongue tip. The deep fibers of the exterior bundle decussate with the basioglossus. In adulthood, a few of these fibers may course anteriorly to merge with the genioglossus fibers at the superior mental spine. The deep fibers of the medial bundle decussate with the ceratoglossus. The superficial fibers of the medial bundle pass between basioglossus and ceratoglossus and merge with the inferior longitudinal and transverse muscles. The

Figure 7. Neuromuscular compartments of the hyoglossus. (a) Exterior sagittal view. (b) View from behind. (c) Interior sagittal view. Chondroglossus (gold) originating from the lesser cornu of the hyoid, ceratoglossus (pink) originating from the greater cornu of the hyoid, and basioglossus (mid and dark purple) originating from the body of the hyoid.

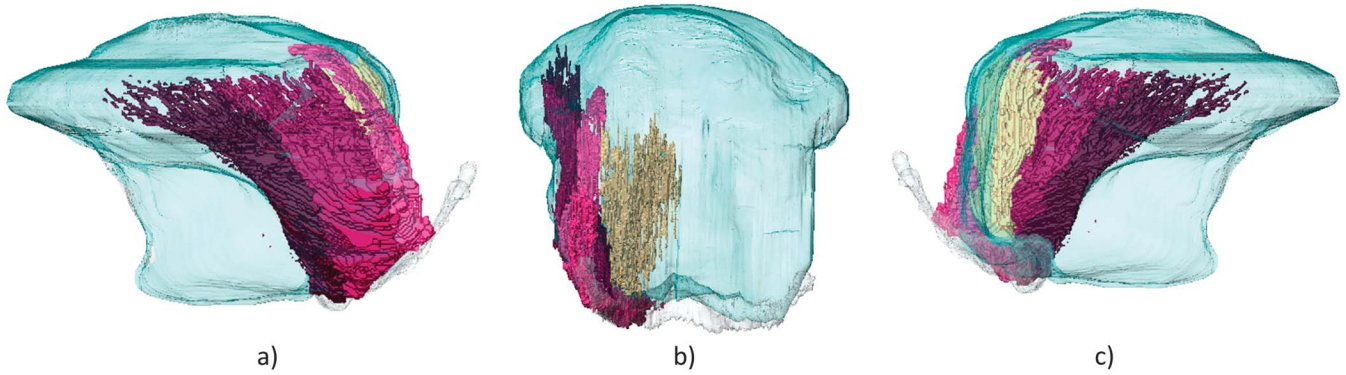

inferior fibers of the interior bundle inserted into the tongue inferior to the insertion of the ceratoglossus. The superficial fibers coursed superiorly to the stylohyoid ligament and attached to it or blended with the lateral fibers of genioglossus.

Mu and Sanders (2010) illustrate primary nerve paths and motor end plates. They indicate a range of motor end plates and nerve branches where the styloglossus joins the tongue body. They also show nerve branches extending along the lateral exterior to innervate the styloglossus in the anterior third of the tongue. This separate location of innervation suggests that rather than a single compartment extending from the styloid process to the tongue tip, the anterior lateral longitudinal fiber bundle has separate functional compartments.

Segmentation of the VHF indicates that the styloglossus can be divided into six bundles extending from the styloid process to the tongue root. Three compartments then enter the tongue body at three different levels (as Sakamoto, 2017, suggests). See Figure 8c for a coronal view of these three compartments from behind the tongue. Figure 9 illustrates how each of these compartments links with a compartment of transversus and genioglossus. There is debate as to whether these intrinsic fiber bundles are styloglossus fibers or transverse fibers, which blend with the styloglossus compartments where they enter the tongue body. The latter structure seems most likely. Of the remaining three compartments, one terminates at the bassioglossus (as Takemoto, 2001, and Barnwell, 1977, suggest), and the other two travel anteriorly and should be regarded as separate lateral longitudinal compartments (as Salter, 1852, suggests). The most superior of these lateral

Figure 8. Neuromuscular compartments of the styloglossus. (a) Axial view from above. (b) View from below. (c) View from behind. Six compartments run from the styloid process to the tongue root. Two anterior lateral compartments (green) are perhaps better thought of as lateral longitudinal compartments complementing the inferior and superior longitudinal compartments. Three compartments are shown coursing medially.

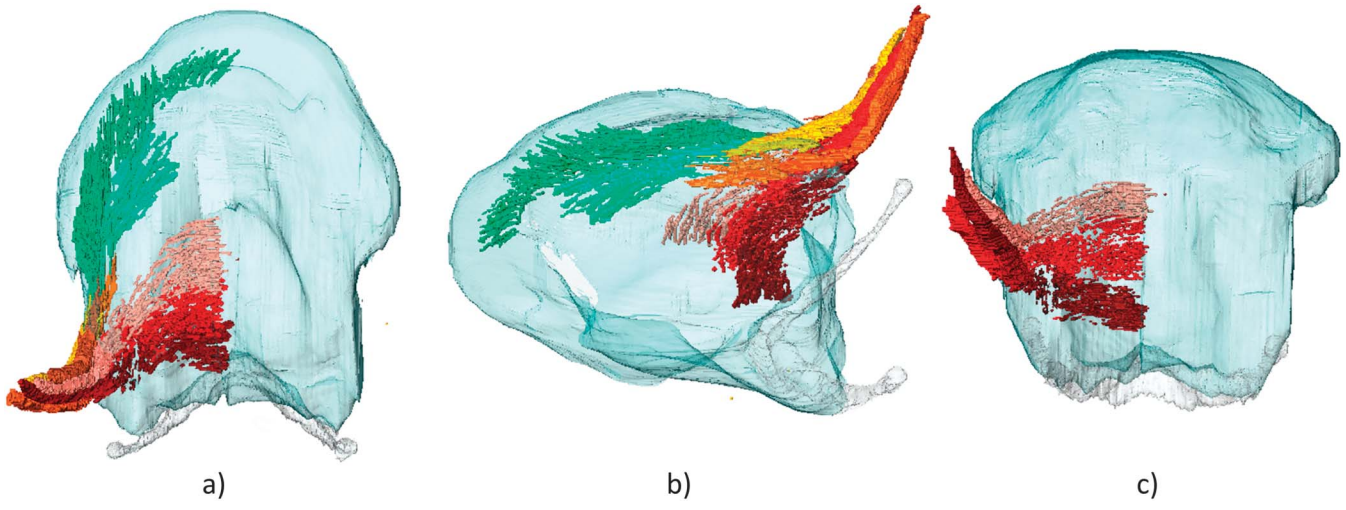

Figure 9. Three neuromuscular compartments of the styloglossus anchor transversus at three different levels corresponding to the three posterior sectors of the genioglossus. (a) Coronal from behind. (b) Axial from above. (c) Sagittal views of a compartment of the styloglossus blending with transverse fibers, which connect with the most posterior genioglossus compartments and the oblique longitudinal compartment. (d) Coronal from behind. (e) Axial from above. (f) Sagittal views of a second compartment of the styloglossus blending with a second set of transverse fibers, which connect with the second most posterior compartments of the genioglossus and the inferior longitudinal compartment. (g) Sagittal and (h) axial from above views of a third compartment of the styloglossus blending with a third set of transverse fibers, which connect with the third most posterior compartments of the genioglossus.

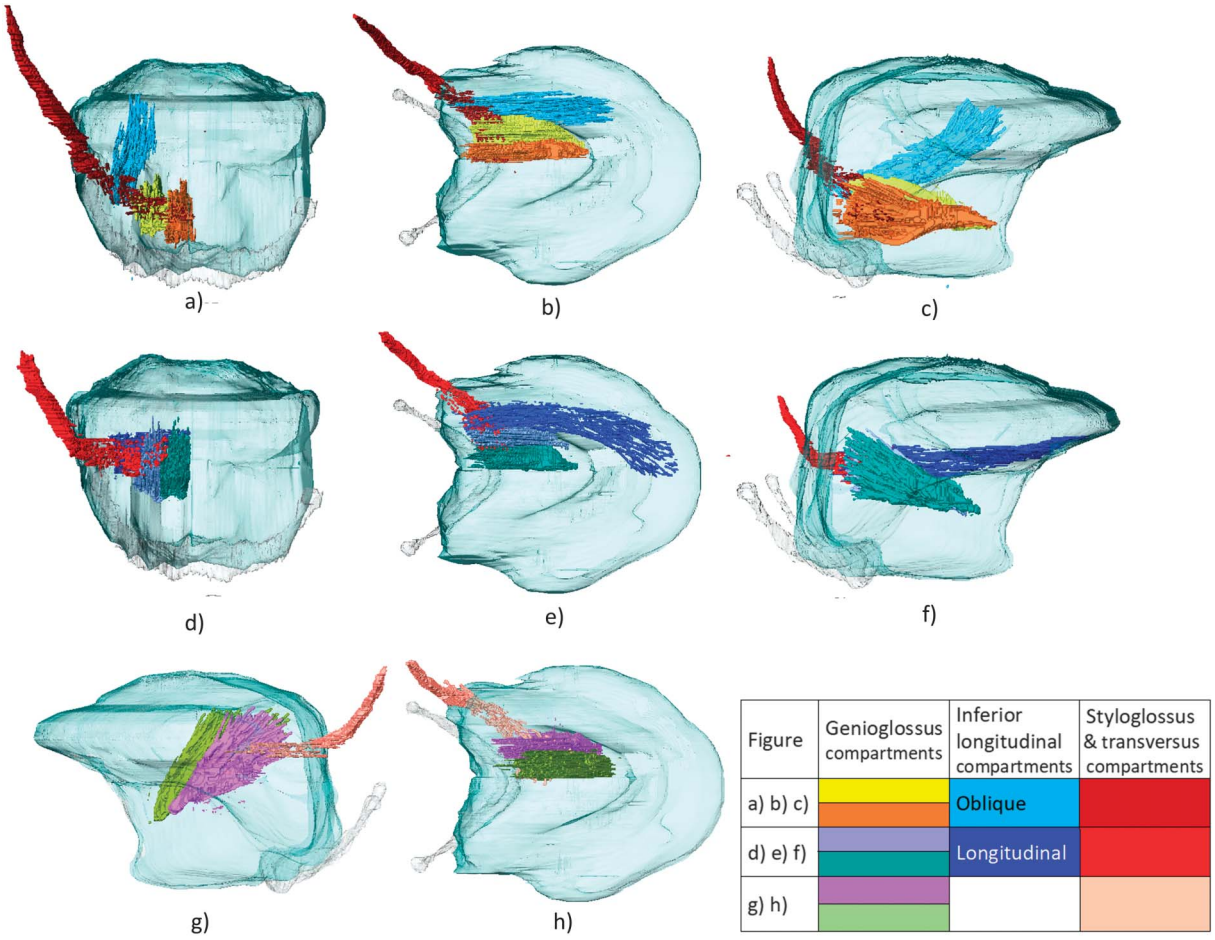

compartments inserts at the tongue tip where it blends with the inferior longitudinal compartment. The second more ventral lateral longitudinal compartment inserts on the ventral surface of the anterior tongue body (see Figure 8).

Palatoglossus and Other External Muscles Attached to the Tongue

It has been asserted (Doménech-Ratto, 1977) that the palatoglossus (see Figure 10, yellow) is a muscle of the tongue that grows during fetal development through the anterior faucal arch into the velum. It proceeds superiorly and anteriorly within the velum. Although officially categorized as a lingual muscle, it is innervated by motor neurons in the nucleus ambiguus, along with other velar muscles and separately from muscles of the tongue, which are innervated by motoneurons in the hypoglossal nucleus. Its line of action and functional description assigns it the ability to raise the tongue. Given the size of the muscle and lack of a rigid origin, this function is unlikely. It is functionally suited to be a palatal constrictor (Klueber et al., 1979). Note that the palatoglossus is a similar size to the proposed compartments of the larger muscles.

The glossopharyngeal compartment of the superior constrictor (see Figure 10, dark green) inserts into the base of the tongue but is not considered as an extrinsic tongue muscle. It is very comparable to the palatoglossus being of approximately equal volume and length to the palatoglossus, with a slightly more posterior attachment to the tongue body. It is functionally a pharyngeal constrictor.

Tonsiloglossus (or amygdaloglossus; see Figure 10, light green) originates within the transverse fiber component

Figure 10. Palatoglossus (yellow), glossopharyngeal compartment of superior constrictor (dark green), palatine tonsil (purple), and tonsilloglossus (light green) shown in (a) sagittal, (b) axial from above, and (c) coronal from behind views.

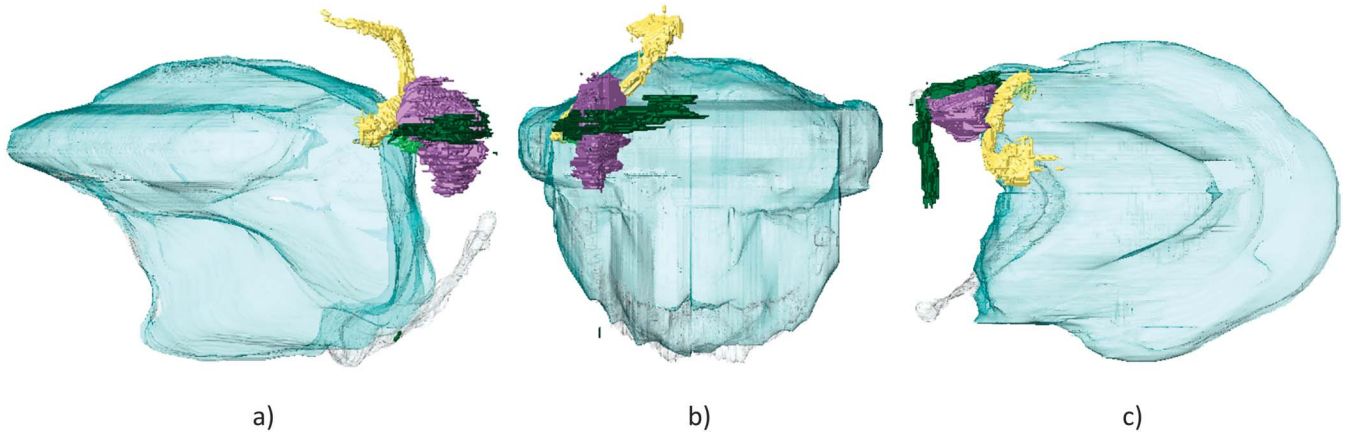

of the tongue and attaches into the inferior half of the lateral aspect of the tonsillar capsule (Rood et al., 1979; see Figure 10, purple). The superior lateral aspect of the tonsillar capsule attaches to the palatopharyngeus. Altogether, the amydaloglossus, palatine tonsil, and palatopharyngeus form a sphincter assisting the glossopharyngeal compartment to constrict the pharynx.

Myloglossus exists in just over half the adult population (Buffoli et al., 2017). It is a very small muscle arising from the mandible and inserting into the tongue root adjacent to or merging with the styloglossus. It was not observed in the VHF.

Inferior Longitudinal

There is evidence that the inferior longitudinal muscle consists of two distinct courses of fibers. Zaglas (1850) observes, "A little beyond its anterior third, its central bundle becomes transversely flattened; sending off radiations from its upper border; the lower following the course of the corresponding border of the stylo-glossus." Albert von Kölliker (1851) observes, "Anteriorly the lingualis inferior unites with the larger bundles of the stylo-glossus; ending at the point of the tongue with them, and also, applying itself anteriorly to the hyo-glossus, it sends many delicate lamellae between the transverse muscles as far as the dorsum of the tongue, presenting, in fact, at the border of the anterior third of the tongue, the same relations as the hyo-glossus further backwards."

Barnwell et al. (1978) divide the muscle in a different way, posterior and anterior parts. They studied 28 human fetuses and observed a posterior part and an anterior part rather than discerning an oblique and longitudinal part. However, Barnwell et al. also note that Oikawa (1973) mentions "upper" and "lower" fibers crossing each other in an X-shaped manner. Saito and Itoh (2003) report in detail that where these fibers cross, they ramify forming a mesh rather than passing each other.

Mu and Sanders (2010) observe separate innervation of a medial and lateral NMC of the inferior longitudinal muscle: "We found that this muscle was composed of two bellies or NMCs arranged in parallel, specifically a lateral (l-IL) and medial (m-IL)." In their article "A Three-Dimensional Atlas of Human Tongue Muscles" (Sanders & Mu, 2013), they describe the two compartments in more detail: "The IL appears to have two parts: a smaller part in the tongue blade lies within the CL and is oriented parallel to the long axis of the tongue; the larger part originates from the hyoid and connective tissue and hyoid medial to the origin of the HG muscle. The larger part courses obliquely straight from the tongue base to the blade without following the curvature of the tongue as the SL does." Sanders et al. (2013) note that the inferior longitudinal muscle does not exhibit a significant difference in fiber type from blade to root.

Segmentation of the VHF indicates two compartments arranged as described by Sanders and Mu (2013). These two compartments are functionally divergent and deserving of separate nomenclature. We will call one part the inferior longitudinal and the other the inferior oblique. The longitudinal part arises in the root of the tongue and inserts at the midsagittal underside of the tongue tip. The oblique part arises at the tongue root slightly inferior and more medial to the longitudinal part and then decussates with the longitudinal part and inserts into the tongue dorsum parasagittally, lateral to the most anterior genioglossus fibers and at two thirds of the distance from the root to the tip.

Contraction of the oblique longitudinal compartment will achieve tongue bunching by restricting the forward protrusion. It can do this without directly changing blade and tip position (see Figure 11). Figure 12a shows

Figure 11. Neuromuscular compartments of inferior longitudinal, inferior oblique (pale blue) and inferior longitudinal (dark blue). (a) Sagittal view. (b) Coronal view from in front. (c) Axial view from above.

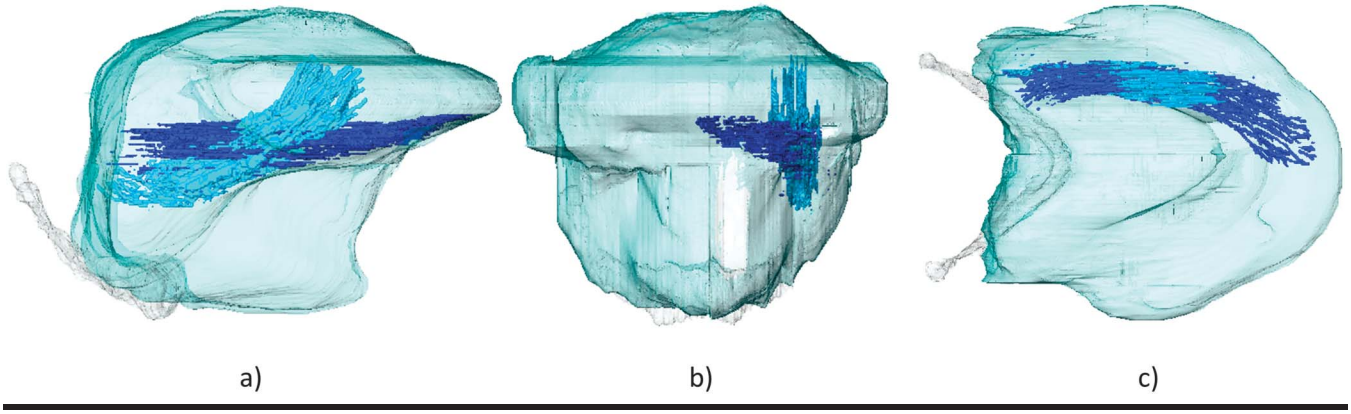

an ultrasound image of bunching, which may be due to contraction of the oblique longitudinal compartment. Figure 12b shows a photograph of a bunched tongue with clear parasagittal dimples where the compartment fibers insert at the dorsum.

Superior Longitudinal

The superior longitudinal muscle is a flat muscular sheet that covers the dorsal surface of the tongue. Slaughter et al. (2005) and Mu and Sanders (2010) observe that it is composed of short fibers each with their own nerve branch and connected in series such that longitudinal sectors of the muscle can be contracted independently. It is observed to be thicker medially and in the middle two fourths longitudinally (Mu & Sanders, 2010; Sakamoto, 2018). Sanders et al. (2013) further note that the composition of fibers in these two regions differs. The medial middle two fourths was largely composed (72%) of slow twitch fibers while the blade had 45% and lateral margins had 50%—the remainder of the fibers being fast twitch.

Figure 12. (a) Sagittal ultrasound image of a child producing a high back vowel and (b) photograph of an adult tongue showing bunching and dimples due to contraction of oblique longitudinal NMC. Arrows show the line of action of this muscle compartment.

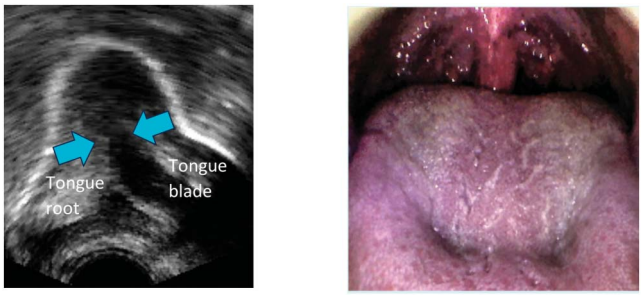

The different composition of fast and slow fibers is an indication that there may be distinct medial and lateral/blade compartments. There is disagreement about the posterior extent of the superior longitudinalis. Barnwell et al. (1978) find fibers only in the anterior two thirds of the tongue body. In fetal tongues, they observe the posterior termination of the superior longitudinalis and the anterior termination of the chondroglossus to be clearly visible at the sulcus terminalis. Others find fibers of the superior longitudinalis extend the entire length of the tongue (Abd-el-Malek, 1939; Iskander & Sanders, 2003; Slaughter et al., 2005). Dabelow (1951) and Barnwell et al. describe a compartmentalization into superior and inferior bundles.

In humans, the hypoglossal nerve sends off four lateral branches before coursing medially at the anterior edge of the hyoglossus. The first of these lateral branches innervates the superior longitudinal muscle. It passes posteriorly to the hyoglossus, reaching the dorsum at the sulcus terminalis. From there, it divides into two to four twigs that course longitudinally. These then send off secondary twigs as they course to the apex. Mu and Sanders (2010) suggest the in-series fiber arrangement and innervation pattern implies NMCs arranged rostrocaudally.

Segmentation of the VHF indicates that the medial fibers tend to curve toward the midsagittal septum while the lateral fibers maintain a longitudinal direction (see Figure 13). This fiber arrangement, along with the distinct fiber type distribution between medial and lateral parts, leads to a proposed arrangement of compartments shown in Figure 13. However, it is likely that there is also compartmentalization longitudinally.

Verticalis and Transversus

The verticalis and transversus fibers course through separate alternating laminae (Takemoto, 2001). The laminae with verticalis fibers also contain the genioglossus

Figure 13. (a) Sagittal view. (b) View from behind. (c) Axial view from above of the superior longitudinal medial compartment (bronze) and lateral/blade compartment (mauve). Chondroglossus (pale gold) and ceratoglossus (cerise) blend with fibers of medial and lateral compartments, respectively.

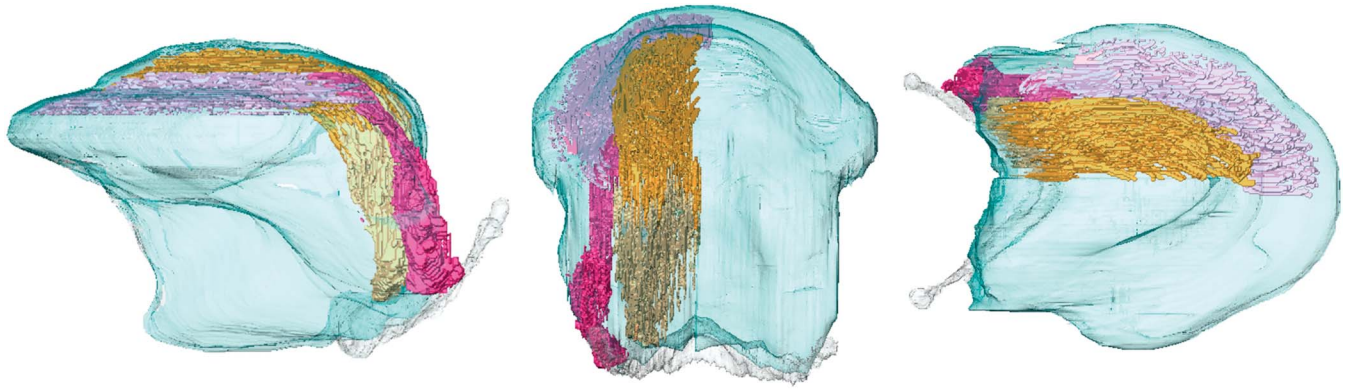

fibers. These laminae radiate from the short tendon so that anteriorly, the laminae lie in the coronal plane, but progressing posteriorly, they align with fibers of the genioglossus such that the laminae lie to a greater extent in the axial plane at the base of the tongue.

Each transverse muscle fiber originates at the midsagittal lingual septum. Long and short fibers terminate at the border and within the body of the tongue, respectively (Sakamoto, 2018). At rest, the transverse fibers form a U-shape within the lamina, the U-shape becoming more pronounced at the tongue root and more horizontal at the tongue blade (see Figure 5). Within each lamina, the deep fibers extend to the lateral margin of the tongue while the superficial ones attach to the dorsum. At the root of the tongue, the transversus merges with fibers of the styloglossus forming a "stirrup" (Honda et al., 2013; Saito & Itoh, 2007). Anterior to the faucal arches, the lateral margin of the tongue is not anchored by styloglossus, and the transversus acts to pull the sides of the tongue medially toward the lingual septum.

Tracing transversus and verticalis fibers in the three orthogonal planes of the VHF was extremely challenging. More versatile segmentation software is required for this purpose. Consequently, an atlas of these muscle compartments is not included here. The myoarchitecture of all the lingual NMCs presented in this article in 2D can be viewed from any angle in 3D at https://sketchfab.com/ArticulateInstruments.

Functional Considerations From Kinematics and Modeling

Kinematic Evidence of Functional Independence of Five Sectors of Genioglossus

An experiment was carried out involving measuring the distance from the short tendon to nine evenly spaced points on the tongue surface from vallecula to tip (Points 1–7, 9, and 11 in Figure 3). Seventeen speakers spoke two utterances each, providing 20,000 ultrasound image frames. Nonspeech parts of recordings were ignored.

All adjacent points are highly correlated in the range of .8–.9. Every second point has moderate correlation of .5–.6, apart from posterior Points 1 and 3 (.7). Every third point is slightly correlated at .2–.4, with again the exception of posterior Points 1 and 4 (.5). More distant points are weakly correlated or uncorrelated at .0–.3. See Figure 14a for an illustration of measurement points and Figure 14b for a tabulation of the correlation coefficients. It is notable that there is no negative correlation between the anterior and posterior parts of the tongue. These results infer that contracting the horizontal compartment of the genioglossus does not cause compartments in the oblique part to extend. Contracting the horizontal compartment may, however, cause rostrocaudal rotation and protrusion. Rotation about the short tendon is not measured here. There is no boundary showing higher correlation within GGh (1–4) and GGo (5–8) than between them (e.g., 4–6). Instead, there is only a proximity effect as should be expected from tissues that are tightly coupled. Correlation cannot determine the exact number of independently controlled compartments, but it is apparent that there are more than two.

A principal component analysis of the data was applied (see Figure 14c). It shows the eigenvectors to be sinusoidal. The first principal component (PC1) has uniform loadings across all variables and would account for different sizes of tongues for the 17 speakers in the data set. PC2 has negative loadings associated with tongue root variables and positive loadings for anterior tongue. This would correspond to an axis of variation from low back through mid back and mid front to high front vowel

Figure 14. (a) Evenly spaced points along the tongue surface selected from nine of the 11 pose-estimated key points. (b) Covariance matrix measuring distances from those nine points on the tongue surface to the short tendon (dotted lines), which shows that neighboring points are correlated but distant points are uncorrelated. Data consisted of 20,000 ultrasound images from 17 speakers producing 34 different sentences. (c) Scree plot of principal component analysis of the data showing no obvious elbow and a plot of the first seven eigenvector loadings, which take the form of sinusoids of increasing frequency.

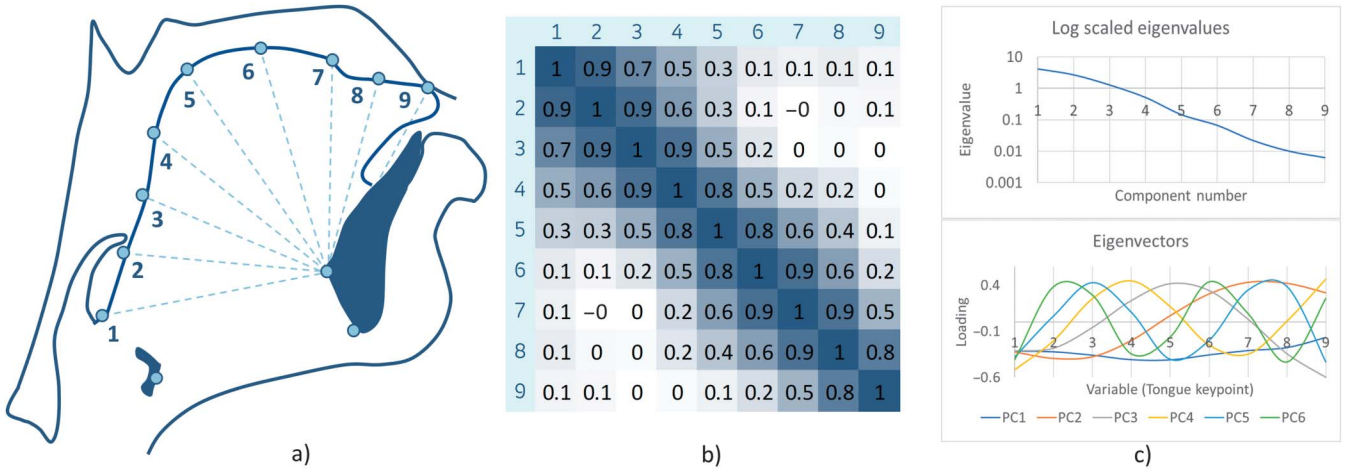

tongue shape, for example. PC3 has a low–high–low loading and would correspond to a high back vowel tongue shape. PC4 might represent a retroflex /r/ shape, while PC5 might represent a bunched /r/ shape. However, caution should be applied to this interpretation as this pattern of sinusoidal components of increasing frequency is what is expected from an approximately Toeplitz correlation matrix (as produced by these data), and this, in turn, is expected when the correlation is due only to the distance between points and not their location. Plotted logarithmically, there is no obvious elbow in the scree plot of eigenvalues (see Figure 14c) to suggest a specific low number of principal components represent the tongue shapes.

In a second experiment, a short utterance was recorded (see Figure 15a), and grooving/doming of the five sectors was measured over time to observe activation patterns. The pose estimation data provide seven points, from the root to the anterior tongue body. For the purpose of this experiment, it was necessary to resample this part of the contour to generate five equidistant points rather than seven. The contour between pose estimation Points 1 and 7 was resampled to 11 points. Then, the resampled Points 2, 4, 6, 8, and 10 were selected to represent the midpoints of each of the five genioglossus sectors (see also Figure 4, lines A, B, C, D, and E). Having automatically extracted these five points, distances from the short tendon to each of the points can be calculated. These distances are charted in Figure 15a and represent doming/grooving in the transverse plane of each of the five sectors. In the following section, a simulation demonstrates the transverse grooving caused by contraction of the genioglossus. It should be emphasized that the distances are not measured along fixed polar axes with origin at the short tendon. The axes will rotate about the short tendon rostrocaudally, as the incompressible sector volumes are compressed coronally and consequently expand rostrocaudally.

In Figure 15a, in the transition period h–k, GG3–GG5 have similar doming patterns, but in transition a–i, they each have distinct patterns. Similarly, in period h–k, GG1–GG3 have different activation patterns, but in period a–i, the patterns for GG1–GG3 are similar. This example shows that the adjacent sectors are often observed to have similar grooving/doming, but they can sometimes be observed to differ. These occasional differences imply the capability to activate five sectors independently.

In a third experiment, a single swallow of a small volume of water was recorded. In Figure 15b, the same five distances are shown for the swallow, as were recorded for the utterance in Experiment 2. The contractions of each genioglossus sector (minima) can be seen to occur in sequence. This corresponds to a peristaltic pattern with a dip in the tongue surface to carry the water bolus from the anterior oral cavity to the posterior pharyngeal cavity. In the anterior three sectors (GG3–GG5), the sector domes immediately after grooving in order to seal the oral cavity once the bolus has passed.

Simulation of Tongue Body Sector Control by Antagonistic Synergy of Genioglossus and Transversus NMCs

Wrench and Balch (2015); Harandi (2015); Harandi, Stavness, et al. (2017); and Harandi, Woo, et al. (2017)

Figure 15. (a) Change in grooving/doming over time for the five sectors GG1–GG5 (see Figure 2) during the utterance /h@kai/. Vertical lines indicate time points where transitions are initiated. Although adjacent sectors often work together, they are all shown to be capable of independent activation patterns. (b) Sequential grooving and doming of the five sectors as a bolus of water is swallowed. NMC = neuromuscular compartment.

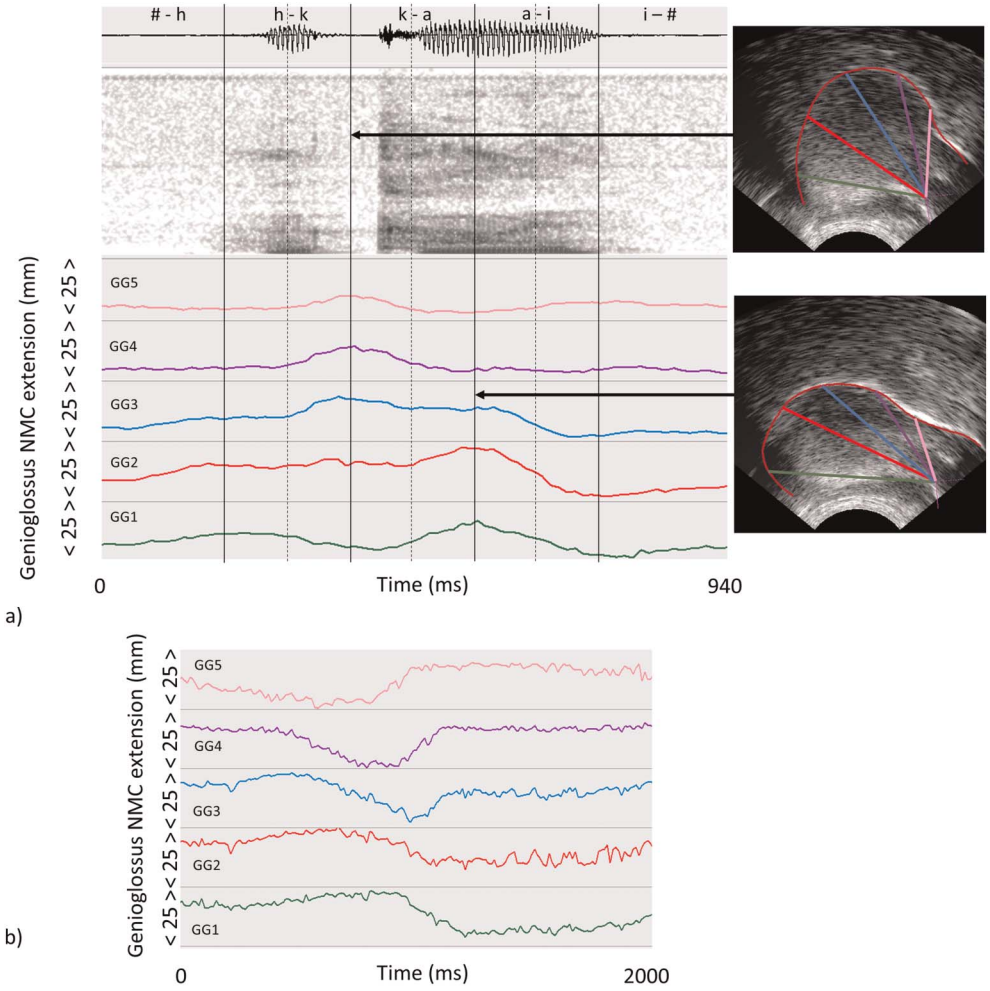

model the tongue by dividing the genioglossus muscle fibers into five functional sectors, referencing (Miyawaki et al., 1975) EMG and nerve stimulation evidence. Muscles actively contract but cannot actively extend so they must work in opposition to allow an action to be reversed. This is as true for the tongue as it is for limb movement. In limb movement, muscles operate around an articulating skeletal structure. In lingual movement, the hydrostatic nature of the intrinsic interweaving muscles preserves volume and thereby provides the necessary structural support. Muscle fibers are aligned orthogonally in longitudinal, transverse, and vertical directions. The maintenance of volume induces extension of fibers in one direction when there is contraction of fibers in two orthogonal directions. In this way, orthogonal NMCs can work in opposition to control shape. In each of the five proposed tongue body sectors, the pair of genioglossus compartments and the verticalis muscle fibers in the associated laminae contract to enlarge the tract cavity at that point. Acting in isovolumetric opposition, the transverse muscle extends the genioglossus and verticalis fibers. A simple biomechanical model (Wrench & Balch, 2015) of the tongue can demonstrate this antagonistic grooving and doming. See the Appendix for a description of this model. Figure 16 demonstrates the shape of a segment at rest (b and f), after genioglossus contraction (c and g), transversus contraction (d and h), and verticalis with genioglossus contraction (e and i). Figures 16f–16i show ultrasound images of comparable coronal cross-sectional shapes produced by articulation of a real tongue.

Discussion

Over the last decade, several prominent scientists have proposed that tongue function is controlled by NMCs

Figure 16. (a) A diagram showing five tongue body sectors pivoting around a short tendon. The fourth sector (pink) is articulated using a simple biomechanical model (Wrench & Balch, 2015) in the following images. (b) Neutral posterior tongue sector shape. (c) Contraction of genioglossus NMCs. (d) Contraction of transversus NMC when the fibers are not fixed at the lateral margins resulting in extension of genioglossus and doming. (e) Verticalis NMCs contract to widen and thin the lateral margins of the tongue body. (f, g, h, i) Ultrasound frames from the same transverse section of the tongue, articulating grooving and doming and demonstrating a range of shapes as produced by the biomechanical model. NMC(s) = neuromuscular compartment(s).

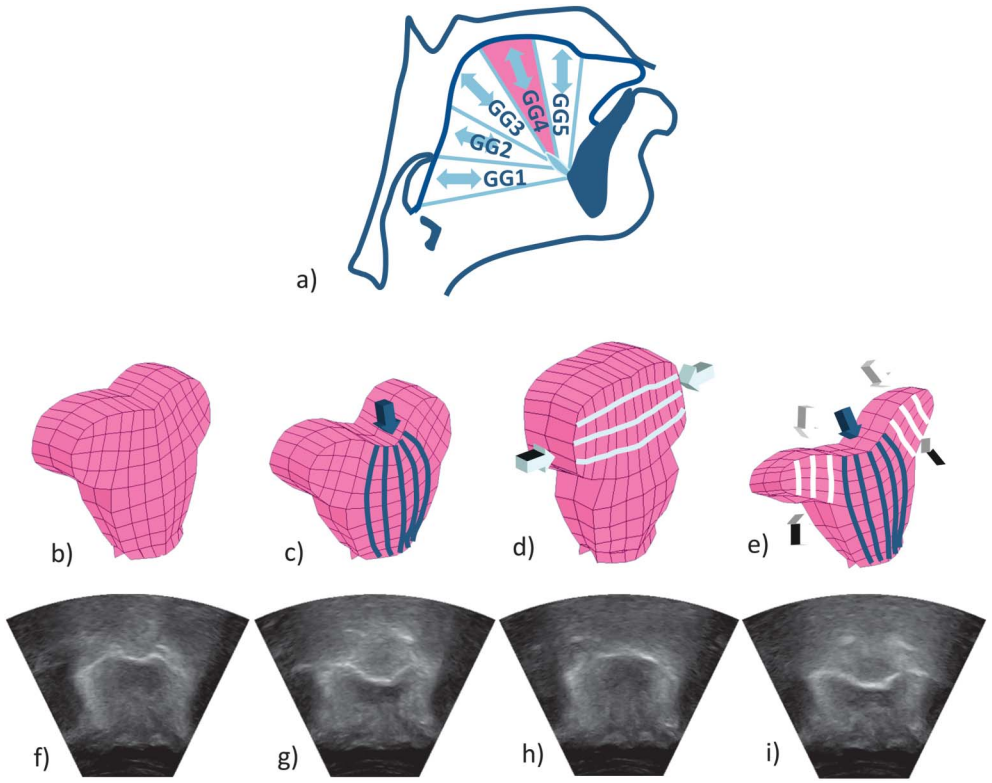

of muscles working in synergistic teams (Bailey, 2011; Liu, 2012; Mu & Sanders, 2010; Sokoloff & Burkholder, 2013). Evidence for a finer functional substrate can be found in many articles, and in this article, an attempt has been made to consolidate these observations into a coherent and functionally plausible myoarchitecture. An atlas of lingual NMCs has been produced by tracing the fibers from the VHF subject with reference to observations of compartments and innervation by various anatomists and histologists. Careful tracing of tongue muscle fibers through the tissues of the VHF subject provides a unique opportunity to picture the course of these fibers in an intact tongue (intact in a digitized space). Crucially, the geometry and intersection of bundles of fibers are preserved, allowing the natural flow of one set of fibers into others to be observed. A functional narrative emerges, which is quite different from the established explanation of tongue movement.

In the fields of phonetics and speech production, linguists consider the tongue body and the tip to be separate articulators. This atlas shows NMCs can be functionally divided into two sets, grouped so that one set controls the tongue body and a second set controls the lateral margin and blade/tip. The tongue body set is shown in Figure 17. The blade and margin set is shown in Figure 18.

The compartments controlling the tongue body include 10 genioglossus compartments arranged in two rows of five pairs such that each pair works with a compartment of transversus and verticalis to control the extent of coronal grooving or doming of a sector of the tongue body. Other compartments controlling the tongue body include a medial superior longitudinal compartment capable of retroflexing the body, an inferior oblique compartment that contracts to bunch the body, and a lateral ventral longitudinal compartment capable of unilaterally pulling the anterior tongue body to one side or bilaterally ventroflexing the tongue body and assisting the inferior oblique in bunching the tongue. Of note, the superior longitudinal muscle has an in-series structure. This means that if one of the genioglossus sectors is contracted so that it expands rostrocaudally, then the short in-series fibers in that sector can stretch independently of other parts of the

Figure 17. How 16 neuromuscular compartments of genioglossus, styloglossus, hyoglossus, and inferior and superior longitudinal muscles relate to each other and due to their course and extent are most likely to control the body shape and position (transversus and verticalis compartments are not shown). (a) Sagittal view. (b) Sagittal view with the basioglossus compartment of the hyoglossus. (c) Axial view from above.

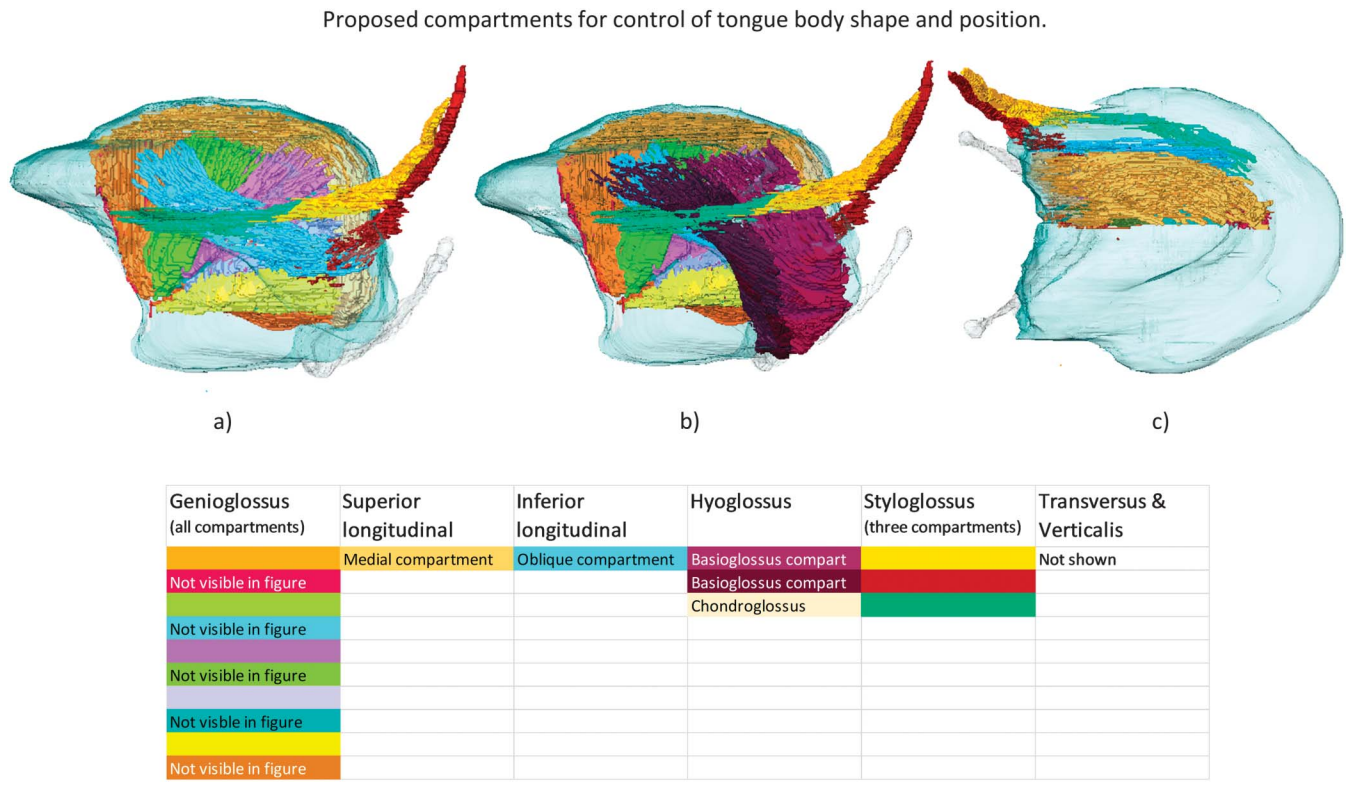

dorsum. Working with these compartments to stabilize the position of their posterior origins are compartments of the styloglossus and chondroglossus (see Figure 17). Since the basioglossus (see Figure 17b) attaches to the lateral margin of the tongue, it is not clear whether it should be included in those compartments controlling the body or the ones controlling the blade and lateral margins. Biomechanical modeling experiments may provide an answer to this question in the future.

The compartments controlling the tongue blade and lateral margins (see Figure 18) include a proposed lateral compartment of the superior longitudinalis muscle, which can act to curl upward the lateral margins and blade; an inferior longitudinal compartment that can act to retract and ventroflex the blade; and a lateral longitudinal compartment of the styloglossus, which can act unilaterally to pull the blade to one side or bilaterally to assist the inferior longitudinal compartment in ventroflexing (uncurling) and retracting the blade. Working with these compartments to stabilize the position of their posterior origins are compartments of the styloglossus and ceratoglossus. Basioglossus may function to uncurl the lateral margins (see Figure 18d).

In the neuromuscular atlas presented here, all of the longitudinal muscle compartments are paired with a muscle compartment of the styloglossus or hyoglossus that is anchored to a bone (see Figures 8, 9, and 13). This arrangement means that an intrinsic muscle compartment can contract to change the shape of the tongue without changing the position of the tongue. As the intrinsic muscle contracts, the anchoring partner can reflexively respond to maintain its length (the stretch reflex). This complicates the interpretation of EMG studies. If an EMG needle is inserted into an anchoring muscle compartment such as the extrinsic part of the styloglossus and reads an activation for a given speech sound, there is no means to tell if this is a volitional excitation to contract that compartment or a reflexive excitation to maintain that compartment's length. There is, of course, also the question of which compartment has been sampled. The compartmentation means the needle placement accuracy has to be more precise than may be practically achievable in most instances.

To take a specific example: There are two possible explanations for EMG activity observed in the production of velar consonants and high back vowels (Waltl & Hoole,

Figure 18. How seven neuromuscular compartments of styloglossus, hyoglossus, and inferior and superior longitudinal muscles relate to each other and due to their course and extent are most likely to control the lateral margin and blade/tip (transversus and verticalis compartments are not shown). (a) Sagittal view. (b) Axial view from above. (c) Axial view from below. (d) Sagittal view including the basioglossus compartment of the hyoglossus, which inserts into the lateral margin of the tongue body.

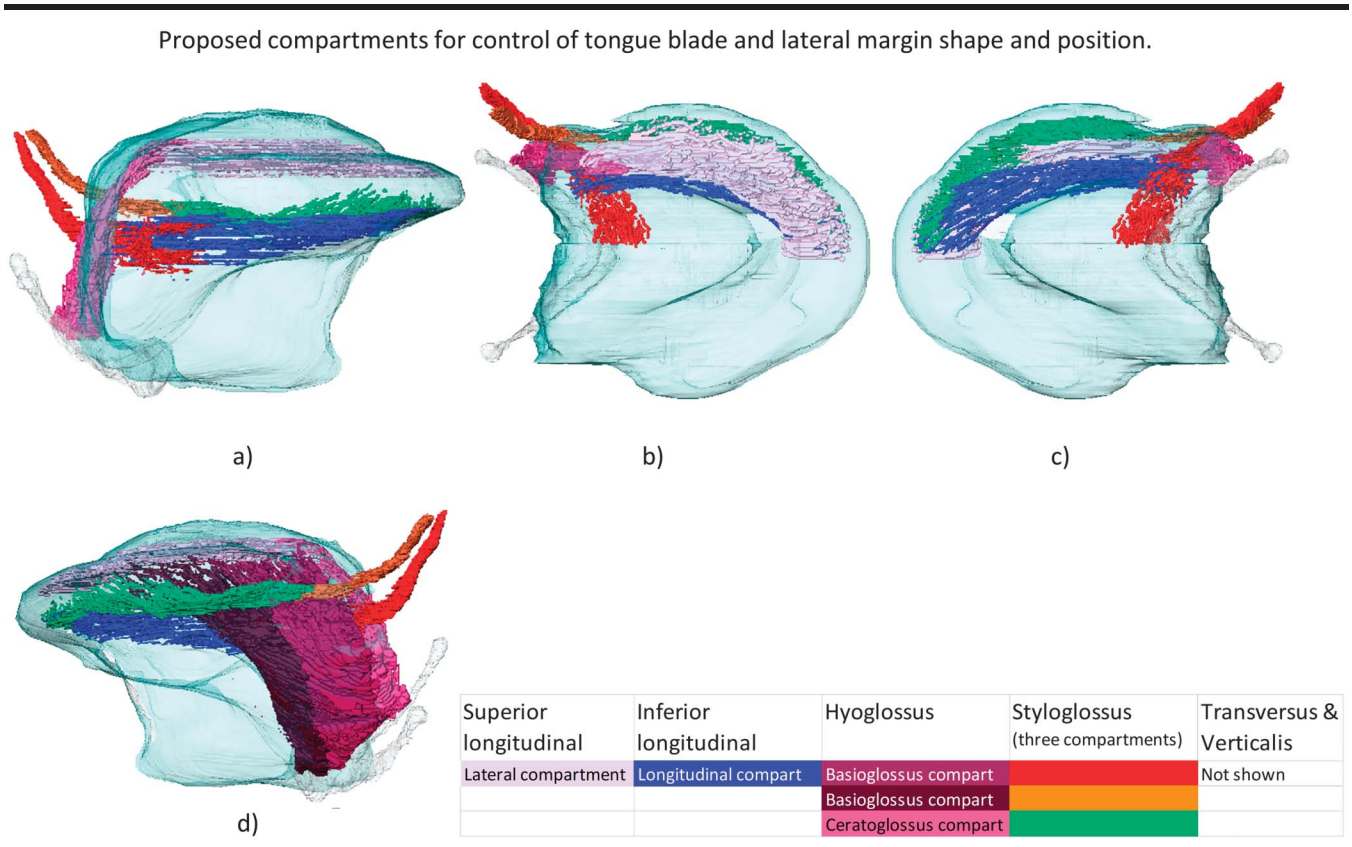

2008). The first is that the external part of the styloglossus contracts as a whole to pull the posterior lateral margins of the tongue body toward the styloid process. A second possibility is that the transverse muscle fibers of any or all of the posterior compartments of the tongue contract to dome the tongue body and create the high back constriction. In this region (see Figures 5 and 12), the transverse fibers blend with three compartments of the styloglossus. As the transverse fibers contract, they stretch the styloglossus compartments, which, in response, must reflexively contract to counter the applied force and maintain their length. Ross et al. (2023) have shown that in one macaque, the styloglossus was strongly active during tongue body retraction, but it did not shorten, which is consistent with the latter hypothesis.

There is at least one further potentially important muscle that has not been considered in detail here: The geniohyoid muscle is not generally considered to be a muscle of the tongue. However, the motoneurons of this muscle are located in the hypoglossal nucleus, along with the tongue muscles. This would imply that it is linked very directly with other lingual compartments via nucleus interneurons. In a swallow action, hyoid advancement, by contraction of the geniohyoid, follows the sequential contraction of the genioglossus compartments. The necessity to coordinate the timing of bolus transfer and airway protection by hyoid advancement may be the reason geniohyoid motoneurons are found in the hypoglossal nucleus. This association raises the possibility that hyoid advancement by this muscle is also an active speech articulator.

The number of independently controlled genioglossus compartments has never been determined. Most often in respiratory studies, it is divided in two, which allows the posterior horizontal fibers to be assigned as a tongue "protrudor." This study finds the strongest evidence in number of nerve twigs and number of distinct fiber bundle origins for five independently controlled sectors, each sector having a pair of compartments. Since the midsagittal tongue shape is important for articulating a range of vowel and consonant sounds, two kinematic studies were carried out. The first study looked at midsagittal distances from the short tendon to points along the tongue surface and concludes that although neighboring points are strongly correlated, anterior and posterior points are

uncorrelated. Previous work by Stone et al. (2004) also examined correlation of points along the tongue surface. In one experiment, they took five phonetically balanced sentences recorded once by one speaker. They selected five points in the middle 50% of the tongue surface, omitting the tongue root and tip (equivalent to Points 4–8 of this nine-point study). Contrary to results presented here, they found strong negative correlation between distant sectors implying that contraction of any posterior sector is associated with extension of all the anterior sectors. From this, they conclude that the tongue has two active regions. However, they note that correlations derived from a single sentence show different points correlating for different phonemes. They see this as a sign of different segments being linked for different phonetic targets. A second experiment in this article confirmed this observation. The second kinematic experiment in this article shows, as Stone et al. (2004) observed, neighboring sectors often have similar activations, but for different phones, the sectors that correlate differ. This experiment demonstrates that at least five sectors are capable of independent activation. It should be noted that nerve stain studies showed fewer than 10 primary nerve twigs serving the genioglossus of some subjects. An interspeaker variation in the exact number of genioglossus compartments is possible.

Some of the early ideas about synergies were proposed by Sherrington (1906), who conceived the muscle synergies as resulting from the activation of specific reflex pathways. Bernstein (1996) also proposed the concept of synergies. He regarded synergies as a way for the central nervous system to deal with the many degrees of freedom that are involved in the generation of movement. A synergy in Bernstein's terms is a means to reduce the number of mechanical variables involved in the execution of even the simplest movement.

In this work, we have investigated synergies between NMCs of the genioglossus and transversus using a simple biomechanical model; we have taken the point of view that this combination of co-activated NMCs operates as a modular neuromuscular structure. Speculatively, each structure could provide agonist/antagonist function. The individual components are linked at a level of the medial hypoglossal nucleus via interneurons, allowing reflexive response between the components. These low-level networks have the potential to permit, for example, the delay of motoneuron activation of antagonist compartments to minimize jerk that would otherwise occur due to simultaneous activation of agonist and antagonist fascicles. Simple biomechanical modeling supports the idea that a pair of genioglossus compartments can work with a compartment of transversus to dome and groove a sector of the tongue body. The coronal cross-sectional domed and grooved shapes produced by the biomechanical model (see Figures 16b–16e) are visually similar to the coronal images of a real tongue imaged by ultrasound (see Figures 16f–16i).

Interindividual differences in tongue volume and at-rest shape clearly exist, and there is some variation in the observed number of primary nerve branches that innervate the genioglossus. It is known that some individuals can roll and fold the tongue while others cannot easily do so but may sometimes be able to after practice. It is not clear the extent to which the functional description presented here might vary depending on these factors. Biomechanical modeling may be one way to investigate how function changes when at-rest muscle compartment volume and fiber course are altered. It is quite easy with the simple biomechanical model introduced here to alter the mesh shape and the course of struts representing muscle fibers.

The proposed compartmental myoarchitecture has implications for our understanding of the speech and swallowing functions. The sequential doming and grooving of the five tongue sectors shown in Figure 15b provides an efficient peristaltic mechanism for propelling a bolus as part of the swallowing action. One can speculate that this may in fact be the primary function of this sector-based structure. For speech production, a motor command to set the relative contraction of the genioglossus and transversus within each sector specifies the amount of grooving of each sector and so provides a simple and direct means to shape the tongue for the production of lax vowels. High front and low back tense vowels may also be directly shaped in this way but require a greater level of muscle contraction to achieve the necessary grooving and doming in each sector. High back vowels may though require additional contraction of inferior longitudinal compartments to constrain rostrocaudal rotation and enlarge the front cavity by lowering the blade and tip. Inserting EMG hook wire electrodes accurately into five different regions of the genioglossus is very challenging. The method, introduced in this article, of estimating EMA-type key points along the whole length of the tongue and at the attachment point of the short tendon provides a new means by which to study genioglossus muscle contractions for different vowels and consonants and during swallowing. It can be used to measure both grooving and doming of tongue body sectors and any rostrocaudal rotation. It is possible to observe, for example, how grooving of posterior compartments co-occurs with rotation of the more anterior compartments about the origin of the short tendon, producing often observed curved (or looping) trajectories. The timing of doming maxima and grooving minima indicates the instants when compartments initiate contraction toward an intended articulatory target, offering insight into how phones are sequenced. It can reveal how speech is not underlyingly segmental but rather a series of transitions. This cannot easily be done with EMA as the short

tendon position is unknown and sensors cannot be attached to the posterior half of the tongue. Importantly for the advancement of our understanding of speech motor control, if we can measure the degree of grooving of each sector over time, it provides a means to monitor indirectly the output of motor commands to this key speech articulator. The strongest evidence presented in this study for the proposed compartments of the tongue arises from the course of muscle fibers and location of primary nerve branches. Going forward, EMG studies might be designed to add to the single study by Miyawaki et al. (1975) where multiple electrodes are inserted to determine whether or not independent activation of different regions of the genioglossus and styloglossus can be observed. It is possible that more precise techniques can be developed for tracing axons from the motoneurons in the hypoglossal nucleus to tightly defined regions of tongue muscles. These would be possible ways to validate and encourage the adoption and/or modification of this proposed functional myoarchitechture.

Data Availability Statement

The visible human male and female data sets are available at https://datadiscovery.nlm.nih.gov/Images/Visible-Human-Project/ux2j-9i9a/about_data. The ultrasound data set used for kinematic analysis is available at https://ultrasuite.github.io/data/tal_corpus/.

References

Abd-el-Malek, S. (1938). A contribution to the study of the movements of the tongue in animals, with special reference to the cat. *Journal of Anatomy, 73*(Pt. 1), 15–30.1.

Abd-el-Malek, S. (1939). Observations on the morphology of the human tongue. *Journal of Anatomy, 73*(Pt. 2), 201–210.3.

Ackerman, M. J. (1998). The visible human project. *Proceedings of the IEEE, 86*(3), 504–511. https://doi.org/10.1109/5.662875

Agur, A. M., & Dalley, A. F. (2005). *Grant's atlas of anatomy* (11th ed.). Lippincott Williams & Wilkins.

Aldes, L. D. (1995). Subcompartmental organization of the ventral (protrusor) compartment in the hypoglossal nucleus of the rat. *Journal of Comparative Neurology, 353*(1), 89–108. https://doi.org/10.1002/cne.903530109

Anderson, P., Fels, S., Harandi, N. M., Ho, A., Moisik, S., Sánchez, C. A., Stavness, I., & Tang, K. (2017). FRANK: A hybrid 3D biomechanical model of the head and neck. In Y. Payan & J. Ohayon (Eds.), *Biomechanics of living organs* (Vol. 1, pp. 413–447). Academic Press. https://doi.org/10.1016/B978-0-12-804009-6.00020-1

Baer, T., Alphonso, P. J., & Honda, K. (1988). Electromyography of the tongue muscles during vowels in /@pVp/ environment. *Annual Bulletin RILP, 22,* 7–19.

Bailey, E. F. (2011). Activities of human genioglossus motor units. *Respiratory Physiology & Neurobiology, 179*(1), 14–22. https://doi.org/10.1016/j.resp.2011.04.018

Baker, T. A. (2008). *A biomechanical model of the human tongue for understanding speech production and other lingual behaviors* [Doctoral dissertation, The University of Arizona].

Barnwell, Y. M. (1977). The morphology of musculus styloglossus in fifteen-week human fetuses. *International Journal of Orofacial Myology and Myofunctional Therapy, 3*(2), 8–46. https://doi.org/10.52010/ijom.1977.3.2.2

Barnwell, Y. M., Klueber, K., & Langdon, H. L. (1978). The anatomy of the intrinsic musculature of the tongue in the early human fetus: Part 1. M. Longitudinalis Superior. *International Journal of Orofacial Myology and Myofunctional Therapy, 4*(3), 5–8. https://doi.org/10.52010/ijom.1978.4.3.1

Bernstein, N. A. (1996). On dexterity and its development. In M. L. Latash, & T. Turvey (Eds.), *Dexterity and its development* (pp. 1–44). Lawrence Erlbaum Associates.

Bizzi, E., & Cheung, V. C. K. (2013). The neural origin of muscle synergies. *Frontiers in Computational Neuroscience, 7,* Article 51. https://doi.org/10.3389/fncom.2013.00051

Buffoli, B., Ferrari, M., Belotti, F., Lancini, D., Cocchi, M. A., Labanca, M., Tschabitscher, M., Rezzani, R., & Rodella, L. F. (2017). The myloglossus in a human cadaver study: Common or uncommon anatomical structure? *Folia Morphologica, 76*(1), 74–81. https://doi.org/10.5603/FM.a2016.0044

Chanaud, C. M., Pratt, C. A., & Loeb, G. E. (1991). Functionally complex muscles of the cat hindlimb. *Experimental Brain Research, 85*(2), 300–313. https://doi.org/10.1007/BF00229408

Crooke, H. (1615). *Mikrocosmographia, a description of the body of man.*

Cruveilhier, J. (1844). *The anatomy of the human body*. Harper & Brothers. https://doi.org/10.5962/bhl.title.40727

Dabelow, R. (1951). Vorstudien zu einer Betrachtung der Zunge als funktionelles System [Preliminary studies in consideration of the tongue as a functional system]. *Morphologisches Jahrbuch, 91,* 33–76.

Dang, J., & Honda, K. (1997). Acoustic characteristics of the piriform fossa in models and humans. *The Journal of the Acoustical Society of America, 101*(1), 456–465. https://doi.org/10.1121/1.417990

Davies, D. V., & Gray, H. (1967). *Gray's anatomy: Descriptive and applied.* Longmans.

Delaey, P., Duisit, J., Behets, C., Duprez, T., Gianello, P., & Lengelé, B. (2017). Specific branches of hypoglossal nerve to genioglossus muscle as a potential target of selective neurostimulation in obstructive sleep apnea: Anatomical and morphometric study. *Surgical and Radiologic Anatomy, 39*(5), 507–515. https://doi.org/10.1007/s00276-016-1778-7

Doménech-Ratto, G. (1977). Development and peripheral innervation of the palatal muscles. *Acta Anatomica, 97*(1), 4–14. https://doi.org/10.1159/000144712

English, A. W., & Weeks, O. (1984). Compartmentalization of single muscle units in cat lateral gastrocnemius. *Experimental Brain Research, 56*(2), 361–368. https://doi.org/10.1007/BF00236292

English, A. W., Wolf, S. L., & Segal, R. L. (1993). Compartmentalization of muscles and their motor nuclei: The partitioning hypothesis. *Physical Therapy, 73*(12), 857–867. https://doi.org/10.1093/ptj/73.12.857

Federative International Programme for Anatomical Terminology. (2019). *Terminologia anatomica* (*2nd ed.*). https://FIPAT.library.dal.ca

Fritzell, B. (1969). The velopharyngeal muscles in speech. An electromyographic and cineradiographic study. *Acta Oto-Laryngologica, 250,* 1–78.

Gérard, J.-M., Wilhelms-Tricarico, R., Perrier, P., & Payan, Y. (2003). *A 3D dynamical biomechanical tongue model to study speech motor control*. PsyArXiv. https://doi.org/10.48550/arXiv.physics/0606148

Gick, B., & Stavness, I. (2013). Modularizing speech. *Frontiers in Psychology, 4,* Article 977. https://doi.org/10.3389/fpsyg.2013.00977

Harandi, M. N. (2015). *3D subject-specific biomechanical modeling and simulation of the oral region and airway with application to speech production* [Doctoral dissertation, The University of British Columbia]. UBC Theses and Dissertations. https://doi.org/10.14288/1.0300338

Harandi, M. N., Stavness, I., Woo, J., Stone, M., Abugharbieh, R., & Fels, S. (2017). Subject-specific biomechanical modelling of the oropharynx: Towards speech production. *Computer Methods in Biomechanics and Biomedical Engineering: Imaging & Visualization, 5*(6), 416–426. https://doi.org/10.1080/21681163.2015.1033756

Harandi, M. N., Woo, J., Stone, M., Abugharbieh, R., & Fels, S. (2017). Variability in muscle activation of simple speech motions: A biomechanical modeling approach. *The Journal of the Acoustical Society of America, 141*(4), 2579–2590. https://doi.org/10.1121/1.4978420

Hermant, N., Perrier, P., & Payan, Y. (2017). Human tongue biomechanical modeling. In Y. Payan & J. Ohayon (Eds.), *Biomechanics of living organs: Hyperelastic constitutive laws for finite element modeling* (pp. 395–411). Elsevier. https://doi.org/10.1016/B978-0-12-804009-6.00019-5

Hirose, H., Kiritani, S., Ushijima, T., & Kjellin, O. (1979). Lingual electromyography related to tongue movements in Swedish vowel production. *Journal of Phonetics, 7*(4), 317–324. https://doi.org/10.1016/S0095-4470(19)31066-6

Honda, K., Murano, E. Z., Takano, S., Masaki, S., & Dang, J. (2013). Anatomical considerations on the extrinsic tongue muscles for articulatory modeling. *Proceedings of Meetings on Acoustics, 19,* Article 060270.

Iskander, A., & Sanders, I. (2003). Morphological comparison between neonatal and adult human tongues. *Annals of Otology, Rhinology & Laryngology, 112*(9), 768–776. https://doi.org/10.1177/000348940311200905

Jonnesco, T. (1902). *Traité d'anatomie humaine* [Treatise on human anatomy] (ed. by P. Poirier, Vol. 4).

Kajee, Y., Pelteret, J. P., & Reddy, B. D. (2013). The biomechanics of the human tongue. *International Journal for Numerical Methods in Biomedical Engineering, 29*(4), 492–514. https://doi.org/10.1002/cnm.2531

Klueber, K. M., Langdon, H. L., & Barnwell, Y. (1979). The morphology of the vertical and transverse intrinsic musculature of the tongue in the 15-week human fetus. *Acta Morphologica Neerlando-Scandinavica, 17*(4), 301–310.

Koelliker, A., Scherer, I., Virchow, R., & Scanzonl, F. (1851). *Verhandlungen der Physikalisch-Medisinischen Gesellschaft zu Würzburg* [Proceedings of the Würzburg Physical-Medical Society] (Vol. 2).

Kuehn, D. P., & Azzam, N. A. (1978). Anatomical characteristics of palatoglossus and the anterior faucial pillar. *The Cleft Palate Journal, 15*(4), 349–359.

Liang, X., Elsaid, N. M., Jiang, L., Roys, S., Puche, A. C., Gullapalli, R. P., Stone, M., Prince, J. L., & Zhuo, J. (2022). Validation of muscle fiber architecture of the human tongue revealed by diffusion magnetic resonance imaging with histology verification. *Journal of Speech, Language, and Hearing Research, 65*(10), 3661–3673. https://doi.org/10.1044/2022_JSLHR-22-00040

Liu, Z.-J. (2012). Tongue muscle response to neuromuscular diseases and specific pathologies. In L. McLoon & F. Andrade (Eds.), *Craniofacial muscles: A new framework for understanding the effector side of craniofacial muscle control* (pp. 241–262). Springer. https://doi.org/10.1007/978-1-4614-4466-4_14

Lubker, J., Salinard, J. B., & May, K. (1973). Palatoglossus function in normal speech production—Electromyographic implications. *The Journal of the Acoustical Society of America, 53*(Suppl. 1), 296. https://doi.org/10.1121/1.1982187

Malpighi, M. (1665). *Tetras Anatomicarum Epistolarum De Lingua, Et Cerebro*. Typis HH. Victorij Benatij.

McClung, J. R., & Goldberg, S. J. (1999). Organization of motoneurons in the dorsal hypoglossal nucleus that innervate the retrusor muscles of the tongue in the rat. *The Anatomical Record, 254*(2), 222–230. https://doi.org/10.1002/(SICI)1097-0185(19990201)254:2<222::AID-AR8>3.0.CO;2-B

McClung, J. R., & Goldberg, S. J. (2002). Organization of the hypoglossal motoneurons that innervate the horizontal and oblique components of the genioglossus muscle in the rat. *Brain Research, 950*(1–2), 321–324. https://doi.org/10.1016/S0006-8993(02)03240-7

Miyawaki, K., Hirose, H., Ushijima, T., & Sawashimi, M. (1975). A preliminary report on the electromyographic study of the lingual muscles. *Annual Bulletin RILP, 9,* 91–106.

Morley, M. E. (1972). *The development and disorders of speech in childhood*. Churchill Livingstone.

Mu, L., & Sanders, I. (1999). Neuromuscular organization of the canine tongue. *The Anatomical Record, 256*(4), 412–424. https://doi.org/10.1002/(SICI)1097-0185(19991201)256:4<412::AID-AR8>3.0.CO;2-5

Mu, L., & Sanders, I. (2010). Human tongue neuroanatomy: Nerve supply and motor endplates. *Clinical Anatomy, 23*(7), 777–791. https://doi.org/10.1002/ca.21011

Nath, T., Mathis, A., Chen, A. C., Patel, A., Bethge, M., & Mathis, M. W. (2019). Using DeepLabCut for 3D markerless pose estimation across species and behaviors. *Nature Protocols, 14*(7), 2152–2176. https://doi.org/10.1038/s41596-019-0176-0

Ogata, S., Mine, K., Tamatsu, Y., & Shimada, K. (2002). Morphological study of the human chondroglossus muscle in Japanese. *Annals of Anatomy-Anatomischer Anzeiger, 184*(5), 493–499. https://doi.org/10.1016/S0940-9602(02)80087-5

Oikawa, R. (1973). Studies on the disposition and distribution of the tongue muscle in human fetus. *Shika Gakuho, 73*(3), 485–527.

O'Kusky, J. R., & Norman, M. G. (1992). Sudden infant death syndrome: Postnatal changes in the numerical density and total number of neurons in the hypoglossal nucleus. *Journal of Neuropathology & Experimental Neurology, 51*(6), 577–584. https://doi.org/10.1097/00005072-199211000-00002

O'Kusky, J. R., & Norman, M. G. (1995). Sudden infant death syndrome: Increased number of synapses in the hypoglossal nucleus. *Journal of Neuropathology & Experimental Neurology, 54*(5), 627–634. https://doi.org/10.1097/00005072-199509000-00003

Pelteret, J. P. V., & Reddy, B. D. (2014). Development of a computational biomechanical model of the human upper-airway soft-tissues toward simulating obstructive sleep apnea. *Clinical Anatomy, 27*(2), 182–200. https://doi.org/10.1002/ca.22313

Rood, S. R., Langdon, H., Klueber, K., & Greenberg, E. (1979). Muscular anatomy of the tonsil and tonsillar bed: A reexamination. *Otolaryngology—Head & Neck Surgery, 87*(4), 401–408. https://doi.org/10.1177/019459987908700402

Ross, C. F., Laurence-Chasen, J., Li, P., Orsbon, C., & Hatsopoulos, N. G. (2023). Biomechanical and cortical control of tongue movements during chewing and swallowing. *Dysphagia, 39,* 1–32. https://doi.org/10.1007/s00455-023-10596-9

Saigusa, H., Niimi, S., Gotoh, T., Yamashita, K., & Kumada, M. (2001). Morphological and histochemical studies of the

genioglossus muscle. *Annals of Otology, Rhinology & Laryngology, 110*(8), 779–784. https://doi.org/10.1177/000348940111000815

Saigusa, H., Yamashita, K., Tanuma, K., Saigusa, M., & Niimi, S. (2004). Morphological studies for retrusive movement of the human adult tongue. *Clinical Anatomy, 17*(2), 93–98. https://doi.org/10.1002/ca.10156

Saito, H., & Itoh, I. (2003). Three-dimensional architecture of the intrinsic tongue muscles, particularly the longitudinal muscle, by the chemical-maceration method. *Anatomical Science International, 78*(3), 168–176. https://doi.org/10.1046/j.0022-7722.2003.00052.x

Saito, H., & Itoh, I. (2007). The three-dimensional architecture of the human styloglossus especially its posterior muscle bundles. *Annals of Anatomy, 189*(3), 261–267. https://doi.org/10.1016/j.aanat.2006.10.002

Sakamoto, Y. (2017). Configuration of the extrinsic muscles of the tongue and their spatial interrelationships. *Surgical and Radiologic Anatomy, 39*(5), 497–506. https://doi.org/10.1007/s00276-016-1777-8

Sakamoto, Y. (2018). Structural arrangement of the intrinsic muscles of the tongue and their relationships with the extrinsic muscles. *Surgical and Radiologic Anatomy, 40*(6), 681–688. https://doi.org/10.1007/s00276-018-1993-5

Sakamoto, Y. (2019). Morphological features of the branching pattern of the hypoglossal nerve. *The Anatomical Record, 302*(4), 558–567. https://doi.org/10.1002/ar.23819

Salter, H. H. (1852). Tongue. In R. B. Todd (Ed.), *The cyclopedia of anatomy and physiology* (Vol. IV, Part II, pp. 1120–1162). Longman, Brown, Green, Longmans, & Roberts.

Sanders, I., & Mu, L. (2013). A three-dimensional atlas of human tongue muscles. *The Anatomical Record, 296*(7), 1102–1114. https://doi.org/10.1002/ar.22711

Sanders, I., Mu, L., Amirali, A., Su, H., & Sobotka, S. (2013). The human tongue slows down to speak: Muscle fibers of the human tongue. *The Anatomical Record, 296*(10), 1615–1627. https://doi.org/10.1002/ar.22755

Schwenk, K. (2001). Extrinsic versus intrinsic lingual muscles: A false dichotomy. *Bulletin of the Museum of Comparative Zoology, 156*(1), 219–235.

Sherrington, C. S. (1906). *The integrative action of the nervous system*. Yale University Press. https://doi.org/10.1037/13798-000

Slaughter, K., Li, H., & Sokoloff, A. J. (2005). Neuromuscular organization of the superior longitudinalis muscle in the human tongue. 1. Motor endplate morphology and muscle fiber architecture. *Cells, Tissues, Organs, 181*(1), 51–64. https://doi.org/10.1159/000089968

Sokoloff, A. J. (1993). Topographic segregation of genioglossus motoneurons in the neonatal rat. *Neuroscience Letters, 155*(1), 102–106. https://doi.org/10.1016/0304-3940(93)90683-C

Sokoloff, A. J., & Burkholder, T. (2013). Tongue structure and function. In L. K. McLoon & F. H. Andrade (Eds.), *Craniofacial muscles: A new framework for understanding the effector side of craniofacial muscle control* (pp. 207–227). Springer.

Sokoloff, A. J., & Deacon, T. W. (1992). Musculotopic organization of the hypoglossal nucleus in the cynomolgus monkey, *Macaca fascicularis*. *Journal of Comparative Neurology, 324*(1), 81–93. https://doi.org/10.1002/cne.903240107

Spitzer, V., Ackerman, M. J., Scherzinger, A. L., & Whitlock, D. (1996). The visible human male: A technical report. *Journal of the American Medical Informatics Association, 3*(2), 118–130. https://doi.org/10.1136/jamia.1996.96236280

Standring, S. (2021). *Gray's anatomy e-book: The anatomical basis of clinical practice*. Elsevier.

Stone, M., Epstein, M. A., & Iskarous, K. (2004). Functional segments in tongue movement. *Clinical Linguistics & Phonetics, 18*(6–8), 507–521. https://doi.org/10.1080/02699200410003583

Stone, M., Woo, J., Lee, J., Poole, T., Seagraves, A., Chung, M., Kim, E., Murano, E. Z., Prince, J. L., & Blemker, S. S. (2018). Structure and variability in human tongue muscle anatomy. *Computer Methods in Biomechanics and Biomedical Engineering: Imaging & Visualization, 6*(5), 499–507. https://doi.org/10.1080/21681163.2016.1162752

Sutlive, T. G., McClung, J. R., & Goldberg, S. J. (1999). Whole-muscle and motor-unit contractile properties of the styloglossus muscle in rat. *Journal of Neurophysiology, 82*(2), 584–592. https://doi.org/10.1152/jn.1999.82.2.584

Takano, S., & Honda, K. (2007). An MRI analysis of the extrinsic tongue muscles during vowel production. *Speech Communication, 49*(1), 49–58. https://doi.org/10.1016/j.specom.2006.09.004

Takemoto, H. (2001). Morphological analyses of the human tongue musculature for three-dimensional modeling. *Journal of Speech, Language, and Hearing Research, 44*(1), 95–107. https://doi.org/10.1044/1092-4388(2001/009)

Taylor, E. N., Hoffman, M. P., Aninwene, G. E., II, & Gilbert, R. J. (2015). Patterns of intersecting fiber arrays revealed in whole muscle with generalized Q-space imaging. *Biophysical Journal, 108*(11), 2740–2749. https://doi.org/10.1016/j.bpj.2015.03.061

Tubbs, R. S., Shoja, M. M., & Loukas, M. (2016). *Bergman's comprehensive encyclopedia of human anatomic variation*. Wiley. https://doi.org/10.1002/9781118430309

Uemura, M., Matsuda, K., Kume, M., Takeuchi, Y., Matsushima, R., & Mizuno, N. (1979). Topographical arrangement of hypoglossal motoneurons: An HRP study in the cat. *Neuroscience Letters, 13*(2), 99–104. https://doi.org/10.1016/0304-3940(79)90024-7

Uemura-Sumi, M., Itoh, M., & Mizuno, N. (1988). The distribution of hypoglossal motoneurons in the dog, rabbit and rat. *Anatomy and Embryology, 177*(5), 389–394. https://doi.org/10.1007/BF00304735

Uemura-Sumi, M., Mizuno, N., Nomura, S., Iwahori, N., Takeuchi, Y., & Matsushima, R. (1981). Topographical representation of the hypoglossal nerve branches and tongue muscles in the hypoglossal nucleus of macaque monkeys. *Neuroscience Letters, 22*(1), 31–35. https://doi.org/10.1016/0304-3940(81)90280-9

Verheyen, P. (1710). *Corporis humani anatomia* [Anatomy of the human body] (Vol. 2). t'Serstevens.

Waltl, S., & Hoole, P. (2008). An EMG study of the German vowel system. *8th International Seminar on Speech Production*. Inria.

Wilhelms-Tricarico, R. (2000). Development of a tongue and mouth floor model for normalization and biomechanical modeling. *Proceedings of the 5th Speech Production Seminar and CREST Workshop on Models of Speech Production, Kloster Seeon*.

Windhorst, U., Hamm, T. M., & Stuart, D. G. (1989). On the function of muscle and reflex partitioning. *Behavioral and Brain Sciences, 12*(4), 629–645. https://doi.org/10.1017/S0140525X00024985

Woo, J., Xing, F., Stone, M., Green, J., Reese, T. G., Brady, T. J., Wedeen, V. J., Prince, J. L., & El Fakhri, G. (2019). Speech map: A statistical multimodal atlas of 4D tongue motion during speech from tagged and cine MR images. *Computer Methods in Biomechanics and Biomedical Engineering: Imaging & Visualization, 7*(4), 361–373. https://doi.org/10.1080/21681163.2017.1382393

Wrench, A., & Balch-Tomes, J. (2022). Beyond the edge: Markerless pose estimation of speech articulators from ultrasound and camera images using DeepLabCut. *Sensors, 22*(3), 1133. https://doi.org/10.3390/s22031133

Wrench, A. A., & Balch, P. (2015). Towards a 3D tongue model for parameterising ultrasound data. *Proceedings of the 18th ICPhS, Glasgow*.

Yeung, J., Burke, P. G. R., Knapman, F. L., Patti, J., Brown, E. C., Gandevia, S. C., Eckert, D. J., Butler, J. E., & Bilston, L. E. (2022). Task-dependent neural control of regions within human genioglossus. *Journal of Applied Physiology, 132*(2), 527–540. https://doi.org/10.1152/japplphysiol.00478.2021

Zaglas, J. (1850). On the muscular structure of the tongue of man, and certain of the mammalia. Part I and Part II. The muscular actions. In J. Goodsir (Ed.), *Annals of anatomy and physiology* (pp. 1–20, 113–126). Edinburgh. https://archive.org/details/b21689465

Appendix (p. 1 of 2)

A Simple Biomechanical Model

The established technique for biomechanical modeling of musculature is the finite element method (FEM) combined with a multibody method used for rigid structures such as bones (Anderson et al., 2017). The FEM was originally developed to model stresses in shaped passive materials under applied force in disciplines such as structural engineering and aeronautical engineering. Consequently, finite element modeling software has mature tools for simulating material properties and for performing stress and strain analysis. Development of tongue models using this technique places emphasis on the modeling of the mechanical properties of passive muscle tissue and constitutive models that best describe the passive tissue response to different mechanical loading conditions. The constitutive model formulates the governing equations that define the stress–strain relations, together with the conservation laws and kinematic relations. Such models are validated by measuring stress–strain relations in real-tongue tissue and comparing the results to those predicted by the model. Less focus is placed on accurately modeling the course of the complex interweaving, independently innervated, muscle fiber bundles. A 600-element polyhedral mesh used for 3D tongue modeling studies was built by Gérard et al. (2003) based on observation of the VHF. It has a number of structural compromises to ensure reasonable FEM computation time and robustness. This mesh is not arranged so that the genioglossus extends from the short tendon, but instead its origin is distributed along the mandible. The mesh therefore does not pivot about the short tendon. The model is only six polyhedrons in width, and their orientation does not match that of the transversus and verticalis muscle fibers of a real tongue. This resolution is too low to allow the mesh to flatten, groove, and cup like a real tongue. A more recent model (Hermant et al., 2017) uses a much finer mesh derived from the same surface structure but with many more internal elements (> 6,000). The lines of force corresponding to muscle activations follow a similar pattern to the Gérard et al. model, although the three genioglossus compartments are realigned to converge at a single point on the mandible. The model is reported to deform in a similarly limited manner to the earlier Gérard et al. model.

The simple model (Wrench & Balch, 2015) used in this article seeks to place the emphasis on modeling of muscle fiber courses in an effort to investigate the effect on tongue shapes more easily. We developed software that allows a complex hexahedral mesh to be generated and edited manually. The software is also designed to allow evaluation by comparison with real-tongue deformations as measured by ultrasound, electropalatography, and electromagnetic articulography. An example tongue model mesh has more than 1,400 hexahedrons with a width of 12. The advantage of this modeling method is that the mesh shape can be edited with relative ease and without risk of simulation failure due to discretization or locking errors. The incompressibility of muscle tissue is modeled by applying a gas pressure calculation inside each hexahedron to maintain its volume. We shape the mesh so that the struts forming the edges of the hexahedra follow, as far as possible, the observed course of muscles in the VHF. Contraction force is applied along these struts. Muscle force is formulated according to a simplified stretch reflex. The nominal length of each strut forming a muscle, expressed as a percentage of the rest length, is used to control the model. In a series of iterative calculations, the nominal muscle length is compared to the current length. If the nominal length is shorter than the actual length, then a contracting force is applied proportional to that difference. The strut forces and volume-preserving pressure forces iterate until an equilibrium is reached. The method is stable and does not lock up or crash, even with complex meshes. It has several limitations. This model does not include mass, inertia, or gravity and so does not realistically model the dynamics of tongue movement. Forces propagating to points distant from the contracting muscle take longer to reach equilibrium than forces applied locally. There is no collision modeling. The model has symmetry imposed about a midsagittal plane. Thus, the midline of the tongue is constrained to lie in this plane. Rigid bodies such as the mandible and hyoid rotate and translate symmetrically about this plane. A given tongue model can be evaluated by manually adjusting muscle lengths to fit the midsagittal profile of the model to selected frames of a movie of midsagittal ultrasound of a speech utterance. The model can be further evaluated by measuring the distance from the model surface to a palatal surface and comparing the model-generated tongue–palate distance patterns to electropalatography patterns recorded of the same utterance by the same speaker. Evaluation may also be performed by tracking the movements of virtual "sensors" placed on the model and comparing their movement to that of data recorded by electromagnetic articulography. The results of one such electropalatography comparison are shown in Figure A1. The MyoSim3D software application can be found, along with sample models and the source code, at https://github.com/articulateinstruments/Biomechanical-Modelling. Users of the software may adjust nominal muscle compartment lengths to see how the tongue model deforms. Users wishing to develop their own model can edit existing models to, for example, alter the resting shape or muscle fiber allocations and so investigate the functional changes that occur as a result. It is envisaged that once a satisfactory model has been developed, the knowledge gained may support development of models with superior kinematic properties in other simulation environments such as finite element modeling.

Appendix (p. 2 of 2)

A Simple Biomechanical Model

Figure A1. Results of fitting the simple biomechanical model to midsagittal ultrasound and comparing the resulting palatal distance pattern to that generated by electropalatography (EPG).